

SEMI-EXPLICIT DISCRETIZATION SCHEMES FOR WEAKLY-COUPLED ELLIPTIC-PARABOLIC PROBLEMS

R. ALTMANN[†], R. MAIER[†], B. UNGER[‡]

ABSTRACT. We prove first-order convergence of the semi-explicit Euler scheme combined with a finite element discretization in space for elliptic-parabolic problems which are weakly coupled. This setting includes poroelasticity, thermoelasticity, as well as multiple-network models used in medical applications. The semi-explicit approach decouples the system such that each time step requires the solution of two small and well-structured linear systems rather than the solution of one large system. The decoupling improves the computational efficiency without decreasing the convergence rates. The presented convergence proof is based on an interpretation of the scheme as an implicit method applied to a constrained partial differential equation with delay term. Here, the delay time equals the used step size. This connection also allows a deeper understanding of the weak coupling condition, which we accomplish to quantify explicitly.

Key words. elliptic-parabolic problem, semi-explicit time discretization, delay, poroelasticity, multiple-network
AMS subject classifications. 65M12, 65L80, 65M60, 76S05

1. INTRODUCTION

We study the semi-explicit time discretization of a linear elliptic problem that is coupled to a linear parabolic equation, which we refer to as *elliptic-parabolic problem*. The resulting model is a partial differential-algebraic equation (PDAE) that appears, for instance, in the field of geomechanics [Bio41, Zob10]. In particular, we consider the deformation of porous media saturated by an incompressible viscous fluid, also called *poroelasticity* [DC93, Sho00]. The displacement of a material due to temperature changes gives a second application, which is commonly known as *thermoelasticity* [Bio56]. These applications have in common that the scaling of the coupling term is typically small, which we refer to hereafter as *weakly coupled*.

An alternative formulation of poroelasticity is obtained by introducing the fluid flux, also called *Darcy velocity*, as an additional variable. This so-called *three-field formulation* is used, for instance, in biomechanics to predict the deformation resulting from tumor growth in the brain [RNM⁺03]. This model is advantageous if one is particularly interested in the fluid flux, since no subsequent calculation is needed. Further, it is well-suited for the extension to network structures, which are used, for instance, in medical applications with several pressure variables. As an example, we mention the investigation of cerebral edema, which may occur as a result of an unnatural accumulation of cerebrospinal fluid in the brain (hydrocephalus) [VCT⁺16]. There, the brain is modeled as a poroelastic medium saturated by four fluid networks: one for the high-pressure arteries, one for the low-pressure arterioles and capillaries, one for the cerebrospinal and interstitial fluids, and one for the veins.

Date: September 10, 2019.

As mentioned above, we deal with PDAEs such that a semi-discretization in space yields a differential-algebraic equation (DAE). As an immediate consequence, one cannot use explicit time-integration schemes [KM06]. The current literature mainly considers a time discretization by the implicit Euler scheme. In [EM09, MP17] this is combined with a finite element discretization in space. The performed error analysis is based on a spatial projection, which is related to the corresponding stationary problem and thus coupled. A decoupled projection operator is introduced in [ACM⁺19, FAC⁺19] for heterogeneous poroelasticity. Other spatial discretization schemes such as continuous and discontinuous Galerkin methods are considered in [PW07a, PW07b, PW08]. Numerical methods based on the three-field formulation are discussed, e.g., in [HRGZ17, HK18, HKLP19]. Finally, we mention [Fu19] where higher-order schemes in space and time are investigated.

We emphasize that all mentioned schemes rely on an implicit time discretization. Thus, one needs to solve a large coupled system in each time step. This may be resolved by using a semi-explicit time-stepping method. Such a discretization decouples the elliptic and parabolic equation with the obvious advantage that the system is split into two subsystems with smaller dimensions. Further, the sparsity pattern of the matrices improves such that the construction of block-preconditioners is facilitated [LMW17]. A first attempt in this direction is presented in [WG07] for the three-field model. There, however, an additional inner iteration is necessary to guarantee convergence. For yet another three-field model, [JCLT19] proposes a similar semi-explicit scheme as in the present paper. However, there is no convergence analysis available.

This paper provides theoretical justification for the decoupling of the elliptic and parabolic equation. We prove convergence of the semi-explicit Euler discretization in time combined with any stable spatial discretization of first order. This includes the classical two-field formulation (Theorem 3.9) as well as the multiple-network case if the exchange rates are small enough (Theorem 4.5). Besides suitable regularity assumptions, we require a weak coupling condition, which is motivated and introduced in Section 2. The convergence proof is based on decoupled spatial projections and the observation that the semi-explicit scheme equals the implicit discretization of a related PDAE with delay term. Hereby, the fixed time delay τ equals the step size for the time integration.

The key technique for the convergence result is to prove that the original coupled PDAE and the associated delay PDAE only differ by an order τ , see Proposition 3.2 and Proposition 4.1 for further details. This novel proof technique allows us to establish the expected rates in space and time and an explicit quantification of the weak coupling condition. As an additional benefit from the delay approach, we observe that the weak coupling condition resembles a necessary condition for asymptotic stability of the semi-discretized delay DAE. This fact is also illustrated in the numerical experiments of Section 5, showing that the stated condition is indeed sharp. We foresee that this strategy can be extended to study further time discretization schemes of semi-explicit type.

Notation. Throughout the paper we write $a \lesssim b$ to indicate that there exists a generic constant C , independent of spatial and temporal discretization parameters, such that $a \leq Cb$. Further, we abbreviate Bochner spaces on the time interval $[0, T]$ for a Banach space \mathcal{X} by $L^p(\mathcal{X}) := L^p(0, T; \mathcal{X})$, $W^{k,p}(\mathcal{X}) := W^{k,p}(0, T; \mathcal{X})$, and $H^k(\mathcal{X}) := H^k(0, T; \mathcal{X})$, $p \geq 1$, $k \in \mathbb{N}$.

2. ELLIPTIC-PARABOLIC PROBLEMS

This section is devoted to an introduction to the considered elliptic-parabolic problems. For this, we consider the weak formulation of the classical two-field model as well as three-field and multiple-network systems. To keep the models fairly general we consider abstract formulations and gather all needed assumptions on the functions spaces and the involved bilinear forms. However, we also discuss practical examples for each case. These examples motivate the notion of *weak coupling*, which we specify in terms of the system parameters.

2.1. Two-field formulation. We consider the weak formulation of elliptic-parabolic problems with two unknowns $u: [0, T] \rightarrow \mathcal{V}$ and $p: [0, T] \rightarrow \mathcal{Q}$, where $T < \infty$ denotes the final time and \mathcal{V}, \mathcal{Q} are Hilbert spaces which already include the boundary conditions, see the examples below. In the abstract setting, the solution pair (u, p) should satisfy

$$(2.1a) \quad a(u, v) - d(v, p) = \langle f, v \rangle,$$

$$(2.1b) \quad d(\dot{u}, q) + c(\dot{p}, q) + b(p, q) = \langle g, q \rangle$$

for all test functions $v \in \mathcal{V}$, $q \in \mathcal{Q}$ and sufficiently smooth source terms $f: [0, T] \rightarrow \mathcal{V}^*$, $g: [0, T] \rightarrow \mathcal{Q}^*$. Hereby, \mathcal{V}^* and \mathcal{Q}^* denote the respective dual spaces for \mathcal{V} and \mathcal{Q} and $\langle \cdot, \cdot \rangle$ denotes the duality pairing. Further, we have initial conditions

$$(2.1c) \quad u(0) = u^0 \in \mathcal{V}, \quad p(0) = p^0 \in \mathcal{Q},$$

which need to respect a consistency condition since system (2.1) defines a PDAE. Although system (2.1) is not in the standard semi-explicit form as analyzed in [EM13, Alt15, AH18], the consistency condition is explicitly given by equation (2.1a) and reads

$$a(u^0, v) - d(v, p^0) = \langle f(0), v \rangle$$

for all $v \in \mathcal{V}$. We further assume that both ansatz spaces are part of a Gelfand triple, cf. [Zei90, Ch. 23.4]. For this, we introduce the pivot spaces \mathcal{H}_v and \mathcal{H}_q such that $\mathcal{V}, \mathcal{H}_v, \mathcal{V}^*$ and $\mathcal{Q}, \mathcal{H}_q, \mathcal{Q}^*$ each form a Gelfand triple. A typical example considers Sobolev spaces including the first weak derivative for \mathcal{V}, \mathcal{Q} and standard L^2 -spaces for $\mathcal{H}_v, \mathcal{H}_q$.

For the involved bilinear forms a, b, c , and d we make the following assumptions: the bilinear form $a: \mathcal{V} \times \mathcal{V} \rightarrow \mathbb{R}$ is symmetric, elliptic, and bounded in \mathcal{V} , i.e.,

$$a(u, u) \geq c_a \|u\|_{\mathcal{V}}^2, \quad a(u, v) \leq C_a \|u\|_{\mathcal{V}} \|v\|_{\mathcal{V}}$$

for all $u, v \in \mathcal{V}$. Note that this also defines a norm $\|\cdot\|_a := a(\cdot, \cdot)^{1/2}$, which is equivalent to the \mathcal{V} -norm. Similarly, $b: \mathcal{Q} \times \mathcal{Q} \rightarrow \mathbb{R}$ is symmetric, elliptic, and bounded in \mathcal{Q} , i.e.,

$$b(p, p) \geq c_b \|p\|_{\mathcal{Q}}^2, \quad b(p, q) \leq C_b \|p\|_{\mathcal{Q}} \|q\|_{\mathcal{Q}}$$

for all $p, q \in \mathcal{Q}$, defining the norm $\|\cdot\|_b$, which is equivalent to the \mathcal{Q} -norm. In the examples in mind where \mathcal{V} and \mathcal{Q} are Sobolev spaces, we assume additionally that the elliptic problems corresponding to a and b are H^2 -regular, cf. [Bra07, Sect. II.7]. Note that this includes an implicit condition on the spatial domain on which the bilinear forms are defined.

Further, the bilinear form $c: \mathcal{Q} \times \mathcal{Q} \rightarrow \mathbb{R}$ is symmetric, elliptic, and bounded in the pivot space \mathcal{H}_q , i.e.,

$$c(p, p) \geq c_c \|p\|_{\mathcal{H}_q}^2, \quad c(p, q) \leq C_c \|p\|_{\mathcal{H}_q} \|q\|_{\mathcal{H}_q}$$

for all $p, q \in \mathcal{H}_Q$. Thus, this defines a norm $\|\cdot\|_c$, which is equivalent to the \mathcal{H}_Q -norm. Finally, the coupling is defined through the bilinear form $d: \mathcal{V} \times \mathcal{Q} \rightarrow \mathbb{R}$, which is bounded in terms of

$$d(u, p) \leq C_d \|u\|_{\mathcal{V}} \|p\|_{\mathcal{H}_Q}, \quad d(u, p) \leq \tilde{C}_d \|u\|_{\mathcal{H}_V} \|p\|_{\mathcal{Q}}$$

for all $u \in \mathcal{V}$ and $p \in \mathcal{Q}$. The possibility to choose whether to estimate u or p in the stronger norm will be used in the convergence analysis in Section 3.3.

We emphasize that the assumptions on the bilinear forms a and b imply the elliptic nature of equation (2.1a) and the parabolic nature of equation (2.1b), which are coupled through the bilinear form d . Furthermore, it is sufficient to prescribe an initial condition for p as equation (2.1a) is then uniquely solvable for u^0 .

Remark 2.1 (DAE structure). Since (2.1) represents a PDAE, a spatial discretization with parameter h leads to a DAE. Considering the time derivative of the first equation, the semi-discrete system can be written as

$$\begin{bmatrix} K_a & -D^T \\ D & M_c \end{bmatrix} \begin{bmatrix} \dot{u}_h \\ \dot{p}_h \end{bmatrix} = \begin{bmatrix} 0 & 0 \\ 0 & -K_b \end{bmatrix} \begin{bmatrix} u_h \\ p_h \end{bmatrix} + \begin{bmatrix} \dot{f}_h \\ g_h \end{bmatrix}.$$

Here, K_a and K_b denote the stiffness matrices corresponding to the bilinear forms a and b , respectively, and M_c is the mass matrix resulting from c . Under reasonable assumptions on the spatial discretization, the properties stated above imply that these three matrices are positive definite. Since the block-diagonal part of the matrix on the left is positive definite and the off-diagonal part is skew-symmetric, the matrix on the left is invertible, which implies that the original DAE has index 1, cf. [BCP96, Sect. 2.2]. In other words, only a single time derivative is necessary in order to reformulate the semi-discrete system as an ODE.

Example 2.2 (Poroelasticity). A well-known example, which fits in the framework of this subsection, is the linear poroelasticity problem in a bounded Lipschitz domain $\Omega \subseteq \mathbb{R}^d$ with $d \in \{2, 3\}$, cf. [Bio41, Sho00]. In this application, we seek for the displacement field $u: [0, T] \times \Omega \rightarrow \mathbb{R}$ and the pressure $p: [0, T] \times \Omega \rightarrow \mathbb{R}$. Considering homogeneous Dirichlet boundary conditions, we have

$$\begin{aligned} a(u, v) &:= \int_{\Omega} \sigma(u) : \varepsilon(v) \, dx, & b(p, q) &:= \int_{\Omega} \frac{\kappa}{\nu} \nabla p \cdot \nabla q \, dx, \\ c(p, q) &:= \int_{\Omega} \frac{1}{M} p q \, dx, & d(u, q) &:= \int_{\Omega} \alpha (\nabla \cdot u) q \, dx \end{aligned}$$

with spaces

$$\mathcal{V} := [H_0^1(\Omega)]^d, \quad \mathcal{H}_V := [L^2(\Omega)]^d, \quad \mathcal{Q} := H_0^1(\Omega), \quad \mathcal{H}_Q := L^2(\Omega).$$

The involved parameters include the stress tensor σ (defined by the Lamé coefficients λ and μ), the permeability κ , the Biot-Willis fluid-solid coupling coefficient α , the Biot modulus M , and the fluid viscosity ν . As usual in linear elasticity, $\varepsilon(u)$ denotes the symmetric gradient. The source terms satisfy $f \equiv 0$ and g represents an injection or production process. We emphasize that the ellipticity of the bilinear form a follows from Korn's inequality. The resulting ellipticity constant is given by μ , see e.g. [Cia88, Th. 6.3.4] for details. In many applications the coupling coefficient α is smaller than one and thus much smaller than the Lamé coefficients, see e.g. [DC93, Sect. 3.3.4].

Example 2.3 (Thermoelasticity). Since the linear thermoelastic problem is – in mathematical terms – equivalent to linear poroelasticity, system (2.1) also applies to this case, cf. [Bio56]. Thermoelasticity describes the displacement of a material due to temperature changes. Similar to Example 2.2, the thermal expansion coefficient in the bilinear form d , which is responsible for the coupling, is much smaller than the stress tensor, cf. [CR14].

Motivated from the previous examples, we make the following assumption on the coupling of the elliptic and parabolic equation.

Assumption 2.4 (Weak coupling). We assume a weak coupling through the bilinear form d in the sense that

$$C_d^2 \leq c_a c_c.$$

As already mentioned and indicated in the two examples presented above, this assumption is satisfied in many applications. A detailed list of poroelastic parameters for different stones is given in [DC93].

2.2. Three-field formulation. System (2.1) can also be expressed in a three-field formulation, i.e., with an additional variable reflecting the flux of p . Such a formulation may be beneficial if the flux is of particular interest and serves here as a first step in the direction of network models. For this formulation, we need three spaces, namely \mathcal{V} , \mathcal{Z} , and \mathcal{Q} , and aim to find the three unknowns $u: [0, T] \rightarrow \mathcal{V}$, $y: [0, T] \rightarrow \mathcal{Z}$, and $p: [0, T] \rightarrow \mathcal{Q}$, which satisfy the system

$$(2.2a) \quad a(u, v) - d(v, p) = \langle f, v \rangle,$$

$$(2.2b) \quad (y, z)_{\mathcal{H}_z} - \hat{d}(z, p) = 0,$$

$$(2.2c) \quad d(\dot{u}, q) + c(\dot{p}, q) + \hat{d}(y, q) = \langle g, q \rangle$$

for all test functions $v \in \mathcal{V}$, $z \in \mathcal{Z}$, and $q \in \mathcal{Q}$. The corresponding initial condition reads $p(\cdot, 0) = p^0 \in \mathcal{Q}$, which defines $u^0 \in \mathcal{V}$ through equation (2.2a).

In the three-field formulation, we assume Gelfand triples $\mathcal{V}, \mathcal{H}_v, \mathcal{V}^*$ and $\mathcal{Z}, \mathcal{H}_z, \mathcal{Z}^*$. The space \mathcal{Q} is typically an L^2 -space such that no pivot space is needed or, in other words, $\mathcal{Q} = \mathcal{H}_q$. For the bilinear forms a and c , we have the same assumptions as in the previous subsection. Note, however, that the assumptions on \mathcal{Q} imply that c is now elliptic on \mathcal{Q} . Further, $d: \mathcal{V} \times \mathcal{Q} \rightarrow \mathbb{R}$ is bounded such that

$$d(u, p) \leq C_d \|u\|_{\mathcal{V}} \|p\|_{\mathcal{Q}}$$

for all $u \in \mathcal{V}$ and $p \in \mathcal{Q}$. For the newly introduced bilinear form $\hat{d}: \mathcal{Z} \times \mathcal{Q} \rightarrow \mathbb{R}$ we assume continuity in the sense of

$$\hat{d}(y, p) \leq C_{\hat{d}} \|y\|_{\mathcal{Z}} \|p\|_{\mathcal{Q}}$$

for all $y \in \mathcal{Z}$ and $p \in \mathcal{Q}$.

Example 2.5 (Poroelasticity). We revisit Example 2.2. The corresponding three-field formulation seeks for the displacement u , the fluid flux or Darcy velocity y , and the pore pressure p , cf. [Bio41]. In the strong form the system reads

$$(2.3a) \quad -\nabla \cdot (\sigma(u)) + \nabla(\alpha p) = f,$$

$$(2.3b) \quad y + \frac{\kappa}{\nu} \nabla p = 0,$$

$$(2.3c) \quad -\alpha \nabla \cdot \dot{u} - \frac{1}{M} \dot{p} - \nabla \cdot y = g$$

with an initial condition for p . The natural boundary conditions in this setting are homogeneous Dirichlet boundary conditions for the displacement and homogeneous Neumann boundary conditions for the pressure that can be reformulated as a boundary condition for the fluid flux. In this case, the spaces are given by

$$\mathcal{V} := H_0^1(\Omega)^d, \quad \mathcal{H}_v := [L^2(\Omega)]^d, \quad \mathcal{Z} := H_0(\operatorname{div}, \Omega), \quad \mathcal{H}_z := [L^2(\Omega)]^d, \quad \mathcal{Q} := L^2(\Omega).$$

Here, $H_0(\operatorname{div}, \Omega)$ denotes the space of functions $z \in [L^2(\Omega)]^d$ with $\nabla \cdot z \in L^2(\Omega)$ and $z \cdot n = 0$ on $\partial\Omega$ with unit normal vector n . In order to guarantee uniqueness of the pressure, one often assumes some additional condition such as a vanishing integral. This example fits in the framework of (2.2) with

$$\hat{d}(z, p) := \int_{\Omega} \left(\nabla \cdot \left(\sqrt{\frac{\kappa}{\nu}} z \right) \right) p \, dx.$$

and $(\cdot, \cdot)_{\mathcal{H}_z}$ as the standard L^2 -norm.

At this point, it would be reasonable to consider a similar weak coupling condition as in Assumption 2.4. However, we will discuss this in the following subsection where we extend the three-field model to the multiple-network case.

2.3. Multiple-network systems. The previously introduced three-field formulation can be easily extended to multiple-networks as they are used in certain brain models, see, e.g., [VCT⁺16]. Note, however, that the extension to multiple-networks is also possible for the two-field model.

We consider the following abstract problem: Find $u: [0, T] \rightarrow \mathcal{V}$, $y_i: [0, T] \rightarrow \mathcal{Z}$, and $p_i: [0, T] \rightarrow \mathcal{Q}$ for $i = 1, \dots, m$, which satisfy the system

$$(2.4a) \quad a(u, v) - \sum_{i=1}^m d_i(v, p_i) = \langle f, v \rangle,$$

$$(2.4b) \quad (y_i, z)_{\mathcal{H}_z} - \hat{d}_i(z, p_i) = 0,$$

$$(2.4c) \quad d_i(\dot{u}, q) + c(\dot{p}_i, q) + \hat{d}_i(y_i, q) - \sum_{j \neq i} \beta_{ij}(p_i - p_j, q)_{\mathcal{Q}} = \langle g_i, q \rangle$$

for all test functions $v \in \mathcal{V}$, $z \in \mathcal{Z}$, and $q \in \mathcal{Q}$. Note that equations (2.4b) and (2.4c) have to be considered for $i = 1, \dots, m$ and, thus, represent m equations each. Initial conditions are given by $p_i(\cdot, 0) = p_i^0 \in \mathcal{Q}$ and define $u^0 \in \mathcal{V}$ as before. The assumptions on the spaces and bilinear forms are as in the three-field model of Section 2.2. This means that each of the bilinear forms $d_i: \mathcal{V} \times \mathcal{Q} \rightarrow \mathbb{R}$ and $\hat{d}_i: \mathcal{Z} \times \mathcal{Q} \rightarrow \mathbb{R}$ behave as d and \hat{d} , respectively. The corresponding continuity constants are denoted by C_{d_i} and $C_{\hat{d}_i}$. The presence of additional variables calls for an adjustment of the weak coupling condition.

Assumption 2.6 (Weak coupling, network case). We assume a weak coupling through the bilinear forms d_i in the sense that

$$\sum_{i=1}^m C_{d_i}^2 \leq c_a c_c.$$

Another coupling is described through the parameters β_{ij} in equation (2.4c). In the case where they represent exchange rates from one network to the other, it is reasonable to assume symmetry, i.e., $\beta_{ij} = \beta_{ji}$, cf. [TV11]. Here, however, we only assume that the coupling parameters are sufficiently small.

Assumption 2.7 (Small exchange rates). We assume small exchange rates between the networks, i.e., we assume that

$$\beta := \max_{i,j \in \{1, \dots, m\}} |\beta_{ij}|$$

is small. In particular, we assume that $6\beta(m-1) \leq c_c$.

Remark 2.8. The introduced network model may be easily extended to the case with different ansatz spaces \mathcal{Q}_i and \mathcal{Z}_i for the variables p_i and y_i , respectively. This may be helpful in order to include varying boundary conditions for the different variables.

Remark 2.9 (DAE structure, network case). With the same arguments as in the two-field case, one can show that the semi-discretization of the multiple-network formulation (2.4) is a DAE of index 1. This follows again by the skew-symmetric block structure and only requires the invertibility of the stiffness and mass matrices.

Example 2.10 (Poroelastic brain model). In medical applications, multiple-network poroelastic models of the brain with different pressures to distinguish vessel types can be used to investigate cerebral edema, cf. [VCT⁺16]. This particular model can be described as an extension of the three-field poroelastic formulation with $m = 4$. Thus, the same spaces and variables as in Example 2.5 can be used but with multiple pressures p_i and fluid fluxes y_i , $i = 1, \dots, 4$, in a bounded Lipschitz domain $\Omega \subseteq \mathbb{R}^d$. In this application, no external forces or injections are present ($f \equiv 0$ and $g \equiv 0$) and only hydrostatic pressure gradients drive the system, scaled by very small coupling constants β_{ij} , $i, j = 1, \dots, 4$. Thus, Assumption 2.7 is satisfied. The bilinear forms are chosen as in Example 2.2 except for d_i , \hat{d}_i , which are defined by

$$d_i(v, q) := \int_{\Omega} \alpha_i (\nabla \cdot v) q \, dx, \quad \hat{d}_i(z, q) := \int_{\Omega} \left(\nabla \cdot \left(\sqrt{\frac{\kappa_i}{\nu_i}} z \right) \right) q \, dx.$$

In this medical application, however, inhomogeneous boundary conditions for p_i are considered on two boundary parts (skull and ventricle surface). Thus, additional boundary terms have to be taken into account, see [VCT⁺16].

3. SEMI-EXPLICIT DISCRETIZATION OF THE TWO-FIELD MODEL

For the numerical solution of (2.1), we propose the combination of a *semi-explicit* time discretization with step size τ and a conforming spatial finite element discretization with mesh size h . Thus, we consider a partition of $[0, T]$ with time points $t_n = n\tau$. The fully discretized system then reads

$$(3.1a) \quad a(u_h^{n+1}, v_h) - d(v_h, p_h^n) = \langle f^{n+1}, v_h \rangle,$$

$$(3.1b) \quad d(D_{\tau}u_h^{n+1}, q_h) + c(D_{\tau}p_h^{n+1}, q_h) + b(p_h^{n+1}, q_h) = \langle g^{n+1}, q_h \rangle$$

with test functions $v_h \in V_h$ and $q_h \in Q_h$. Hereby, $V_h \subseteq \mathcal{V}$ and $Q_h \subseteq \mathcal{Q}$ denote suitable finite-dimensional spaces resulting from the spatial discretization. The discrete time derivative is denoted by $D_{\tau}u_h^{n+1} := (u_h^{n+1} - u_h^n)/\tau$ and u_h^n , p_h^n are the resulting approximations of $u(t_n)$ and $p(t_n)$, respectively. For the right-hand sides, we introduce $f^n := f(t_n)$ and $g^n := g(t_n)$. For the initial data, we assume $u_h^0 \in V_h$ and $p_h^0 \in Q_h$ to be consistent in the sense of $a(u^0, v_h) - d(v_h, p_h^0) = \langle f^0, v_h \rangle$.

We emphasize that the scheme (3.1) is semi-explicit in time due to the term p_h^n in equation (3.1a). The corresponding implicit scheme (with p_h^{n+1}) is analyzed in [EM09].

Remark 3.1. The semi-explicit scheme (3.1) may be interpreted as a co-simulation [Mie89, BY11] (also known as waveform relaxation or dynamic iteration) of equations (2.1a) and (2.1b).

The advantage of the proposed scheme over a full-implicit discretization is that we can solve sequentially for u_h^{n+1} by (3.1a) and afterwards for p_h^{n+1} by (3.1b). Hence, we solve two smaller systems rather than one large system in each time step. Further, the sparsity pattern improves, since both systems only include the solution with standard mass and stiffness matrices.

Our convergence proof is based on an elliptic-parabolic problem with an additional delay term whose solution (\bar{u}, \bar{p}) only differs by an order of τ from the original solution (u, p) . The delay system is discussed in the following subsection.

3.1. A related delay system. The semi-explicit scheme (3.1) can also be obtained by applying the *implicit* Euler method to the delay system

$$(3.2a) \quad a(\bar{u}, v) - d(v, \bar{p}(\cdot - \tau)) = \langle f, v \rangle,$$

$$(3.2b) \quad d(\dot{\bar{u}}, q) + c(\dot{\bar{p}}, q) + b(\bar{p}, q) = \langle g, q \rangle$$

for test functions $v \in \mathcal{V}$ and $q \in \mathcal{Q}$. Note that this changes the nature of the system in the sense that we now need a *history function* for \bar{p} in $[-\tau, 0]$ rather than only an initial value. Thus, we set $\bar{p}|_{[-\tau, 0]}(t) = \Phi(t)$ and demand

$$(3.3) \quad \Phi(-\tau) = \Phi(0) = p^0, \quad \Phi \in C^\infty([- \tau, 0], \mathcal{Q}).$$

With this particular history function we have $\bar{p}(0) = \Phi(0) = p^0$ and by equation (3.2a) we conclude $\bar{u}(0) = u^0$, since

$$a(\bar{u}(0), v) = \langle f(0), v \rangle + d(v, \Phi(-\tau)) = \langle f(0), v \rangle + d(v, p^0).$$

Let us emphasize that the time delay equals the temporal step size τ .

Proposition 3.2. *Assume sufficiently smooth right-hand sides f and g and a history function Φ as defined in (3.3) such that the solution (\bar{u}, \bar{p}) of the delay system (3.2) satisfies $\bar{p} \in W^{2,\infty}(\mathcal{H}_Q)$. Then, the solutions to (2.1) and (3.2) are equal up to a term of order τ . More precisely, we have for almost all $t \in [0, T]$ that*

$$\|\bar{p}(t) - p(t)\|_{\mathcal{Q}}^2 \lesssim \tau^2 t (\|\ddot{\Phi}\|_{L^\infty(-\tau, 0; \mathcal{H}_Q)}^2 + \|\ddot{\bar{p}}\|_{L^\infty(\mathcal{H}_Q)}^2)$$

and

$$\|\bar{u}(t) - u(t)\|_{\mathcal{V}}^2 \lesssim \tau^2 \|\dot{\bar{p}}\|_{L^2(\mathcal{H}_Q)}^2 + \tau^2 (1 + \tau^2) t (\|\ddot{\Phi}\|_{L^\infty(-\tau, 0; \mathcal{H}_Q)}^2 + \|\ddot{\bar{p}}\|_{L^\infty(\mathcal{H}_Q)}^2).$$

Proof. We consider the Taylor expansions of \bar{p} and $\dot{\bar{p}}$,

$$(3.4) \quad \bar{p}(t - \tau) = \bar{p}(t) - \tau \dot{\bar{p}}(t) + \frac{1}{2} \tau^2 \ddot{\bar{p}}(\zeta_t), \quad \dot{\bar{p}}(t - \tau) = \dot{\bar{p}}(t) - \tau \ddot{\bar{p}}(\xi_t)$$

for some $\zeta_t, \xi_t \in (t - \tau, t) \subseteq (-\tau, T]$. With this, the differences $e_u := \bar{u} - u$ and $e_p := \bar{p} - p$ satisfy the system

$$(3.5a) \quad a(e_u, v) - d(v, e_p) = -\tau d(v, \dot{\bar{p}}) + \frac{1}{2} \tau^2 d(v, \ddot{\bar{p}}(\zeta_t))$$

$$(3.5b) \quad d(\dot{e}_u, q) + c(\dot{e}_p, q) + b(e_p, q) = 0$$

for all test functions $v \in \mathcal{V}$, $q \in \mathcal{Q}$. Note that we have $e_u(0) = 0$ and $e_p(0) = 0$ due to the particular choice of the history function Φ in (3.3). On the other hand, considering the derivatives of (2.1a) and (3.2a) and the Taylor expansion of $\dot{\bar{p}}$ gives

$$(3.6) \quad a(\dot{e}_u, v) - d(v, \dot{e}_p) = -\tau d(v, \ddot{\bar{p}}(\xi_t)).$$

Taking the sum of (3.6) with test function $v = \dot{e}_u$ and (3.5b) with $q = \dot{e}_p$, we get with the ellipticity of the bilinear forms and Young's inequality,

$$\|\dot{e}_u(t)\|_{\mathcal{V}}^2 + \|\dot{e}_p(t)\|_{\mathcal{H}_Q}^2 + \frac{1}{2} \frac{d}{dt} \|e_p(t)\|_b^2 \lesssim \tau^2 \|\ddot{\bar{p}}(\xi_t)\|_{\mathcal{H}_Q}^2.$$

Thus, we conclude by integration over $[0, t]$ that

$$(3.7) \quad \int_0^t \|\dot{e}_u(s)\|_{\mathcal{V}}^2 ds + \|e_p(t)\|_{\mathcal{Q}}^2 \lesssim \tau^2 t \|\ddot{\bar{p}}\|_{L^\infty(-\tau, t; \mathcal{H}_Q)}^2.$$

Besides, the sum of (3.5a) with $v = \dot{e}_u$ and (3.5b) with $q = e_p$ yields the estimate

$$\begin{aligned} \frac{1}{2} \frac{d}{dt} \|e_u(t)\|_a^2 + \frac{1}{2} \frac{d}{dt} \|e_p(t)\|_c^2 + \|e_p(t)\|_b^2 &= -\tau d(\dot{e}_u(t), \dot{\bar{p}}(t)) + \frac{1}{2} \tau^2 d(\dot{e}_u(t), \ddot{\bar{p}}(\zeta_t)) \\ &\lesssim \|\dot{e}_u(t)\|_{\mathcal{V}}^2 + \tau^2 \|\dot{\bar{p}}(t)\|_{\mathcal{H}_Q}^2 + \tau^4 \|\ddot{\bar{p}}(\zeta_t)\|_{\mathcal{H}_Q}^2. \end{aligned}$$

Integration over $[0, t]$ and application of the estimate (3.7) then leads to

$$\|e_u(t)\|_{\mathcal{V}}^2 \lesssim \tau^2 \|\dot{\bar{p}}\|_{L^2(0, t; \mathcal{H}_Q)}^2 + \tau^2 (1 + \tau^2) t \|\ddot{\bar{p}}\|_{L^\infty(-\tau, t; \mathcal{H}_Q)}^2.$$

Noting that $\ddot{\bar{p}}|_{[-\tau, 0]} = \ddot{\Phi}$ finally completes the proof. \square

The previous result states that the solutions (u, p) and (\bar{u}, \bar{p}) are close as long as the solution of the related delay system stays stable. We would like to point out that the stability of delay PDAEs is a delicate topic, particularly in the current setting where the system structure is of *neutral type*. This means that $\dot{\bar{p}}$ at time t depends on $\dot{\bar{p}}(t - \tau)$. From the PDE side one can expect difficulties, since even delay systems of *retarded type*, where the differential equation only includes a delay of the form $\bar{p}(t - \tau)$, may not gain smoothness in contrast to the finite-dimensional setting [AZ18]. On the other hand, a DAE with a delay term in the constraint may even behave like an *advanced* equation [Cam80], i.e., the solution at time t depends on the derivative of the solution at time $t - \tau$. As a direct consequence one can only expect solutions in a distributional setting [TU19]. Classical solutions may be obtained, if a certain structure is imposed on the delay DAE and the history function satisfies so-called *splicing conditions* [Ung18]. For our particular case, we can prove that $\ddot{\bar{p}}$ indeed stays uniformly bounded for smooth data, see Appendix A for further details.

For an infinite time interval, i.e., $T = \infty$, such a stability result is only possible under a weak coupling condition in the spirit of Assumption 2.4. We illustrate this in the following finite-dimensional example.

Example 3.3. A spatial discretization of the delay PDAE (3.2) can be written as

$$(3.8a) \quad K_a \bar{u}_h(t) - D^T \bar{p}_h(t - \tau) = f_h(t),$$

$$(3.8b) \quad D \dot{\bar{u}}_h(t) + M_c \dot{\bar{p}}_h(t) + K_b \bar{p}_h(t) = g_h(t),$$

with the matrices from Remark 2.1. Solving the first equation for \bar{u}_h and substituting in the second equation results in the neutral delay differential equation

$$(3.9) \quad M_c \dot{\bar{p}}_h(t) + K_b \bar{p}_h(t) = -DK_a^{-1} D^T \dot{\bar{p}}_h(t - \tau) - K_a^{-1} \dot{f}_h(t) + g_h(t).$$

A necessary condition for the *asymptotic stability* of (3.9) is that the spectral radius of $M_c^{-1}DK_a^{-1}D^T$ is strictly smaller than one, see [GKC03, Th. 3.20] for further details. Note that this condition quantitatively resembles the weak coupling condition in Assumption 2.4.

We emphasize that even if \ddot{p} stays bounded for finite times T , it may become very large. A T -independent bound requires again a weak coupling condition, which is also observable numerically, cf. Section 5.3.

3.2. Spatial projection. Based on the two-field formulation (2.1) and discrete spaces V_h and Q_h , we define the projections $R_u: \mathcal{V} \rightarrow V_h$ and $R_p: \mathcal{Q} \rightarrow Q_h$ by

$$(3.10) \quad a(R_u u, v_h) = a(u, v_h)$$

for all $v_h \in V_h$ and

$$(3.11) \quad b(R_p p, q_h) = b(p, q_h)$$

for all $q_h \in Q_h$. Note that R_u and R_p are well-defined due to the ellipticity of a and b . For the following error analysis, we need certain approximation properties of the projectors.

Assumption 3.4 (Spatial projection). Consider $u \in \mathcal{V}$ and $p \in \mathcal{Q}$. We assume that the projection errors satisfy

$$\begin{aligned} \|u - R_u u\|_{\mathcal{H}_v} &\lesssim h \|u\|_{\mathcal{V}}, & \|u - R_u u\|_{\mathcal{V}} &\lesssim h \|\nabla^2 u\|_{\mathcal{H}_v} \\ \|u - R_p p\|_{\mathcal{H}_q} &\lesssim h \|p\|_{\mathcal{Q}}, & \|p - R_p p\|_{\mathcal{Q}} &\lesssim h \|\nabla^2 p\|_{\mathcal{H}_q}, \end{aligned}$$

if the second derivatives $\nabla^2 u$ and $\nabla^2 p$ are bounded in \mathcal{H}_v and \mathcal{H}_q , respectively.

Example 3.5. For the spaces $\mathcal{V} = [H_0^1(\Omega)]^d$, $\mathcal{H}_v = [L^2(\Omega)]^d$, $\mathcal{Q} = H_0^1(\Omega)$, and $\mathcal{H}_q = L^2(\Omega)$, Assumption 3.4 is satisfied if V_h and Q_h equal the standard P_1 Lagrange finite element spaces, see e.g. [Bra07, Ch. II.6-II.7] for more details.

3.3. Full discretization of the delay system. As mentioned above, we prove the convergence of the semi-explicit scheme (3.1) by the interpretation as an implicit discretization of the delay system (3.2). The following proposition quantifies the error estimate between the fully discrete solution and the exact solution to the delay system.

Proposition 3.6. *Suppose Assumptions 2.4 and 3.4 and the assumptions of Proposition 3.2 hold, as well as $\nabla^2 \bar{u} \in L^\infty(\mathcal{H}_v)$ and $\nabla^2 \bar{p} \in L^\infty(\mathcal{H}_q)$. Then, taking initial data $u_h^0 \in V_h$ and $p_h^0 \in Q_h$ with*

$$\|R_u u^0 - u_h^0\|_{\mathcal{V}} + \|R_p p^0 - p_h^0\|_{\mathcal{H}_q} \lesssim h$$

implies that for all $n \leq T/\tau$ the solution of the fully discretized system (3.1) satisfies

$$\|\bar{u}(t_n) - u_h^n\|_{\mathcal{V}}^2 + \|\bar{p}(t_n) - p_h^n\|_{\mathcal{H}_q}^2 + \sum_{k=1}^n \tau \|\bar{p}(t_k) - p_h^k\|_{\mathcal{Q}}^2 \lesssim e^{t_n} (1 + t_n) (h^2 + \tau^2).$$

Before we prove Proposition 3.6, we state the following useful lemma, which is easily proven by straight-forward calculations.

Lemma 3.7. *For a symmetric bilinear form \mathfrak{a} it holds that*

$$2\mathfrak{a}(u, u - v) = \|u\|_{\mathfrak{a}}^2 - \|v\|_{\mathfrak{a}}^2 + \|u - v\|_{\mathfrak{a}}^2$$

with $\|\cdot\|_{\mathfrak{a}}^2 := \mathfrak{a}(\cdot, \cdot)$.

Proof of Proposition 3.6. We follow the ideas presented in [EM09] and introduce

$$\eta_u^n := R_u \bar{u}^n - u_h^n \in V_h \quad \text{and} \quad \eta_p^n := R_p \bar{p}^n - p_h^n \in Q_h,$$

where $\bar{u}^n := \bar{u}(t_n)$ and $\bar{p}^n := \bar{p}(t_n)$ are the solutions of (3.2) and R_u , R_p denote the projections defined in (3.10) and (3.11), respectively. Note, however, that these projections differ from the projections used in [EM09]. Using (3.1a) and (3.2a), we immediately obtain

$$\begin{aligned} a(\eta_u^{n+1}, v_h) - d(v_h, \eta_p^{n+1}) &= a(\bar{u}^{n+1} - u_h^{n+1}, v_h) - d(v_h, R_p \bar{p}^n - p_h^n) - d(v_h, \eta_p^{n+1} - \eta_p^n) \\ &= d(v_h, \bar{p}^n - R_p \bar{p}^n) - d(v_h, \eta_p^{n+1} - \eta_p^n) \end{aligned}$$

for all test functions $v_h \in V_h$. Similarly, we observe that

$$\begin{aligned} \tau b(\eta_p^{n+1}, q_h) &= \tau b(\bar{p}^{n+1} - p_h^{n+1}, q_h) \\ &= -d(\tau \dot{\bar{u}}^{n+1}, q_h) - c(\tau \dot{\bar{p}}^{n+1}, q_h) + d(\tau D_\tau u_h^{n+1}, q_h) + c(\tau D_\tau p_h^{n+1}, q_h) \end{aligned}$$

for all $q_h \in Q_h$. Together with

$$\theta_u^{n+1} := R_u \bar{u}^{n+1} - R_u \bar{u}^n - \tau \dot{\bar{u}}^{n+1} \quad \text{and} \quad \theta_p^{n+1} := R_p \bar{p}^{n+1} - R_p \bar{p}^n - \tau \dot{\bar{p}}^{n+1},$$

this implies

$$\begin{aligned} &d(\eta_u^{n+1} - \eta_u^n, q_h) + c(\eta_p^{n+1} - \eta_p^n, q_h) + \tau b(\eta_p^{n+1}, q_h) \\ &= d(R_u \bar{u}^{n+1} - R_u \bar{u}^n - \tau D_\tau u_h^{n+1}, q_h) + c(R_p \bar{p}^{n+1} - R_p \bar{p}^n - \tau D_\tau p_h^{n+1}, q_h) + \tau b(\eta_p^{n+1}, q_h) \\ &= d(\theta_u^{n+1}, q_h) + c(\theta_p^{n+1}, q_h) \end{aligned}$$

for all $q_h \in Q_h$. For the particular choices $v_h = \eta_u^{n+1} - \eta_u^n$ and $q_h = \eta_p^{n+1}$, we obtain

$$\begin{aligned} &a(\eta_u^{n+1}, \eta_u^{n+1} - \eta_u^n) + c(\eta_p^{n+1} - \eta_p^n, \eta_p^{n+1}) + \tau b(\eta_p^{n+1}, \eta_p^{n+1}) \\ &= d(\eta_u^{n+1} - \eta_u^n, \bar{p}^n - R_p \bar{p}^n - \eta_p^{n+1} + \eta_p^n) + d(\theta_u^{n+1}, \eta_p^{n+1}) + c(\theta_p^{n+1}, \eta_p^{n+1}). \end{aligned}$$

Using Lemma 3.7 for the bilinear forms a and c , we obtain

$$\begin{aligned} &\|\eta_u^{n+1}\|_a^2 - \|\eta_u^n\|_a^2 + \|\tau D_\tau \eta_u^{n+1}\|_a^2 + \|\eta_p^{n+1}\|_c^2 - \|\eta_p^n\|_c^2 + \|\tau D_\tau \eta_p^{n+1}\|_c^2 + 2\tau \|\eta_p^{n+1}\|_b^2 \\ &= 2d(\tau D_\tau \eta_u^{n+1}, \bar{p}^n - R_p \bar{p}^n - \tau D_\tau \eta_p^{n+1}) + 2d(\theta_u^{n+1}, \eta_p^{n+1}) + 2c(\theta_p^{n+1}, \eta_p^{n+1}). \end{aligned}$$

With the identity

$$\begin{aligned} &d(\tau D \eta_u^{n+1}, \bar{p}^n - R_p \bar{p}^n) \\ &= d(\eta_u^{n+1}, \bar{p}^n - R_p \bar{p}^n) - d(\eta_u^n, \bar{p}^{n-1} - R_p \bar{p}^{n-1}) - d(\eta_u^n, (\bar{p}^n - \bar{p}^{n-1}) - R_p(\bar{p}^n - \bar{p}^{n-1})) \end{aligned}$$

and the Taylor expansion $\bar{p}^n - \bar{p}^{n-1} = \dot{\bar{p}}(\xi)$, the weighted version of Young's inequality, cf. [Eva98, App. B], leads to

$$\begin{aligned} &2d(\tau D \eta_u^{n+1}, \bar{p}^n - R_p \bar{p}^n - \tau D \eta_p^{n+1}) \\ &\leq \frac{C_d^2}{c_a c_c} \|\tau D \eta_u^{n+1}\|_a^2 + \|\tau D \eta_p^{n+1}\|_c^2 + \tau \|\eta_u^n\|_a^2 + \tau \frac{C_d^2}{c_a} \|\dot{\bar{p}} - R_p \dot{\bar{p}}\|_{L^\infty(\mathcal{H}_Q)}^2 \\ &\quad + 2d(\eta_u^{n+1}, \bar{p}^n - R_p \bar{p}^n) - 2d(\eta_u^n, \bar{p}^{n-1} - R_p \bar{p}^{n-1}). \end{aligned}$$

Similarly, we obtain for the two other terms

$$2d(\theta_u^{n+1}, \eta_p^{n+1}) \leq \frac{2\tilde{C}_d}{\sqrt{c_b}} \|\theta_u^{n+1}\|_{\mathcal{H}_V} \|\eta_p^{n+1}\|_b \leq \frac{\tilde{C}_d}{c_b} \frac{2}{\tau} \|\theta_u^{n+1}\|_{\mathcal{H}_V}^2 + \frac{\tau}{2} \|\eta_p^{n+1}\|_b^2$$

and with the continuity constant $C_{\mathcal{Q} \hookrightarrow \mathcal{H}_\varepsilon}$ of the embedding $\mathcal{Q} \hookrightarrow \mathcal{H}_\varepsilon$,

$$2c(\theta_p^{n+1}, \eta_p^{n+1}) \leq 2C_c \|\theta_p^{n+1}\|_{\mathcal{H}_\varepsilon} \|\eta_p^{n+1}\|_{\mathcal{H}_\varepsilon} \leq \frac{C_c^2 C_{\mathcal{Q} \hookrightarrow \mathcal{H}_\varepsilon}^2}{c_b} \frac{2}{\tau} \|\theta_p^{n+1}\|_{\mathcal{H}_\varepsilon}^2 + \frac{\tau}{2} \|\eta_p^{n+1}\|_b^2.$$

Next, we combine the previous estimates and absorb the terms $\|\tau D_\tau \eta_p^{n+1}\|_c^2$, $\tau \|\eta_p^{n+1}\|_b$, and $\|\tau D_\tau \eta_u^{n+1}\|_a^2$ using Assumption 2.4 for the latter. Invoking Assumption 3.4 then yields

$$\begin{aligned} (3.12) \quad & \|\eta_u^{n+1}\|_a^2 - (1 + \tau) \|\eta_u^n\|_a^2 + \|\eta_p^{n+1}\|_c^2 - \|\eta_p^n\|_c^2 + \tau \|\eta_p^{n+1}\|_b^2 \\ & - 2d(\eta_u^{n+1}, \bar{p}^n - R_p \bar{p}^n) + 2d(\eta_u^n, \bar{p}^{n-1} - R_p \bar{p}^{n-1}) \\ & \lesssim \tau h^2 \|\dot{\bar{p}}\|_{L^\infty(\mathcal{Q})}^2 + \frac{1}{\tau} \|\theta_u^{n+1}\|_{\mathcal{H}_\varepsilon}^2 + \frac{1}{\tau} \|\theta_p^{n+1}\|_{\mathcal{H}_\varepsilon}^2. \end{aligned}$$

To estimate θ_u^{n+1} and θ_p^{n+1} , we observe

$$\begin{aligned} \theta_u^{n+1} &= \int_{t_n}^{t_{n+1}} R_u \dot{\bar{u}}(s) \, ds - \left((s - t_n) \dot{\bar{u}}(s) \Big|_{t_n}^{t_{n+1}} - \int_{t_n}^{t_{n+1}} \dot{\bar{u}}(s) \, ds \right) - \int_{t_n}^{t_{n+1}} \ddot{\bar{u}}(s) \, ds \\ &= - \int_{t_n}^{t_{n+1}} \dot{\bar{u}}(s) - R_u \dot{\bar{u}}(s) \, ds - \int_{t_n}^{t_{n+1}} (s - t_n) \ddot{\bar{u}}(s) \, ds \end{aligned}$$

and thus, by Assumption 3.4,

$$\|\theta_u^{n+1}\|_{\mathcal{H}_\varepsilon} \leq \int_{t_n}^{t_{n+1}} \|\dot{\bar{u}} - R_u \dot{\bar{u}}\|_{\mathcal{H}_\varepsilon} \, ds + \tau^2 \|\ddot{\bar{u}}\|_{L^\infty(t_n, t_{n+1}; \mathcal{H}_\varepsilon)} \lesssim \tau h \|\dot{\bar{u}}\|_{L^\infty(\mathcal{V})} + \tau^2 \|\ddot{\bar{u}}\|_{L^\infty(\mathcal{H}_\varepsilon)}.$$

Note that the regularity of the history function Φ and $\bar{p} \in W^{2,\infty}(\mathcal{H}_\varepsilon)$ imply $\bar{u} \in W^{2,\infty}(\mathcal{V})$ by (3.2a). In the same manner, we obtain for θ_p^{n+1} the estimate

$$\|\theta_p^{n+1}\|_{\mathcal{H}_\varepsilon} \lesssim \tau h \|\dot{\bar{p}}\|_{L^\infty(\mathcal{Q})} + \tau^2 \|\ddot{\bar{p}}\|_{L^\infty(\mathcal{H}_\varepsilon)}.$$

Taking the sum over n in (3.12), we finally obtain

$$\begin{aligned} & \|\eta_u^n\|_a^2 + \|\eta_p^n\|_c^2 + \sum_{k=1}^n \tau \|\eta_p^k\|_b^2 \\ & \lesssim e^{t_n} \left[h^2 + t_n \left(h^2 \|\dot{\bar{p}}\|_{L^\infty(\mathcal{Q})}^2 + h^2 \|\dot{\bar{u}}\|_{L^\infty(\mathcal{V})}^2 + \tau^2 \|\ddot{\bar{u}}\|_{L^\infty(\mathcal{H}_\varepsilon)}^2 \right. \right. \\ & \quad \left. \left. + h^2 \|\dot{\bar{p}}\|_{L^\infty(\mathcal{Q})}^2 + \tau^2 \|\ddot{\bar{p}}\|_{L^\infty(\mathcal{H}_\varepsilon)}^2 \right) + h^2 \|\bar{p}\|_{L^\infty(\mathcal{Q})}^2 \right] \\ & \lesssim e^{t_n} (1 + t_n) (h^2 + \tau^2). \end{aligned}$$

Note that the exponential factor appears due to the ‘perturbed’ telescope sum in (3.12) and the application of a discrete Grönwall inequality. Finally, using the assumed regularity and Assumption 3.4, i.e.,

$$\|\bar{u}^n - R_u \bar{u}^n\|_{\mathcal{V}} \lesssim h \|\nabla^2 \bar{u}^n\|_{\mathcal{H}_\varepsilon}, \quad \|\bar{p}^n - R_p \bar{p}^n\|_{\mathcal{H}_\varepsilon} \lesssim h \|\bar{p}^n\|_{\mathcal{Q}}, \quad \|\bar{p}^n - R_p \bar{p}^n\|_{\mathcal{Q}} \lesssim h \|\nabla^2 \bar{p}^n\|_{\mathcal{H}_\varepsilon},$$

the assertion follows by the triangle inequality. \square

Remark 3.8. With the same assumptions as in Proposition 3.6 and a slightly stronger coupling condition (namely with a factor $1 + \varepsilon$), one can also show that the considered error is bounded by a constant times $t_n (h^2 + \tau^2 + h^4 \tau^{-1})$. Thus, the exponential term can be exchanged by a higher-order term, which includes the step size τ in the denominator. This, however, is not critical in the range of interest with $\tau \approx h$.

3.4. Convergence of the semi-explicit scheme. We close this section with a summary of the previous results, which states that the semi-explicit scheme (3.1) converges with order $h + \tau$ if the finite element spaces are chosen appropriately and the weak coupling condition is satisfied.

Theorem 3.9 (Convergence, two-field model). *Suppose that Assumptions 2.4 and 3.4 hold. Further, let the right-hand sides $f: [0, T] \rightarrow \mathcal{H}_v$ and $g: [0, T] \rightarrow \mathcal{H}_Q$ be sufficiently smooth. Then, with (u, p) being the solution of the original system (2.1) and $u_h^n \in V_h$, $p_h^n \in Q_h$ the fully discrete approximations obtained by (3.1) for $n \leq T/\tau$ and initial data $u_h^0 \in V_h$, $p_h^0 \in Q_h$ with*

$$\|R_u u^0 - u_h^0\|_{\mathcal{V}} + \|R_p p^0 - p_h^0\|_{\mathcal{H}_Q} \lesssim h,$$

we obtain the error estimate

$$\|u(t_n) - u_h^n\|_{\mathcal{V}}^2 + \|p(t_n) - p_h^n\|_{\mathcal{H}_Q}^2 + \sum_{k=1}^n \tau \|p(t_k) - p_h^k\|_{\mathcal{Q}}^2 \lesssim e^{t_n} (1 + t_n) (h^2 + \tau^2).$$

Proof. If we define the history function Φ as in (3.3), then the assumptions on the data imply that the solution of the related delay system (3.2) stays bounded in the sense of $\bar{p} \in W^{2,\infty}(\mathcal{H}_Q)$, cf. Appendix A. Further, the assumed H^2 -regularity of the bilinear forms a and b yields that $\nabla^2 \bar{u}$ and $\nabla^2 \bar{p}$ are bounded as well, i.e., $\nabla^2 \bar{u} \in L^\infty(\mathcal{H}_v)$ and $\nabla^2 \bar{p} \in L^\infty(\mathcal{H}_Q)$. Thus, all assumptions of Propositions 3.2 and 3.6 are satisfied and the stated estimate directly follows from the previous results and the triangle inequality. Proposition 3.2 shows that the continuous solutions (u, p) and (\bar{u}, \bar{p}) are close, whereas Proposition 3.6 shows that the fully discrete solution approximates the solution of the delay system with the given order. \square

4. SEMI-EXPLICIT DISCRETIZATION OF THE NETWORK MODEL

Similar to the two-field model discussed in Section 3, we now consider a semi-explicit time discretization of the multiple-network system (2.4). Note that this includes the three-field formulation as a special case for $m = 1$. For the network model, the combination of semi-explicit time discretization and conforming spatial discretization leads to

$$(4.1a) \quad a(u_h^{n+1}, v_h) - \sum_{i=1}^m d_i(v_h, p_{i,h}^n) = \langle f^{n+1}, v_h \rangle,$$

$$(4.1b) \quad (y_{i,h}^{n+1}, z_h)_{\mathcal{H}_Z} - \hat{d}_i(z_h, p_{i,h}^{n+1}) = 0,$$

$$(4.1c)$$

$$d_i(D_\tau u_h^{n+1}, q_h) + c(D_\tau p_{i,h}^{n+1}, q_h) + \hat{d}_i(y_{i,h}^{n+1}, q_h) - \sum_{j \neq i} \beta_{ij} (p_{i,h}^{n+1} - p_{j,h}^{n+1}, q_h)_{\mathcal{Q}} = \langle g_i^{n+1}, q_h \rangle$$

for all test functions $v_h \in V_h$, $z_h \in Z_h$, $q_h \in Q_h$ and $i = 1, \dots, m$. As before, we consider a partition of $[0, T]$ with time points $t_n = n\tau$, conforming finite element spaces $V_h \subseteq \mathcal{V}$, $Z_h \subseteq \mathcal{Z}$, $Q_h \subseteq \mathcal{Q}$, and u_h^n , $y_{i,h}^n$, $p_{i,h}^n$ denote the fully-discrete approximations at time t_n .

Throughout this section, we consider the weak coupling condition from Assumption 2.6 as well as the small exchange condition from Assumption 2.7.

4.1. A related network model with delay. We insert a delay term to system (2.4), i.e., we consider the solution $(\bar{u}, \bar{y}_i, \bar{p}_i)$ to

$$(4.2a) \quad a(\bar{u}, v) - \sum_{i=1}^m d_i(v, \bar{p}_i(\cdot - \tau)) = \langle f, v \rangle,$$

$$(4.2b) \quad (\bar{y}_i, z)_{\mathcal{H}_z} - \hat{d}_i(z, \bar{p}_i) = 0,$$

$$(4.2c) \quad d_i(\dot{\bar{u}}, q) + c(\dot{\bar{p}}_i, q) + \hat{d}_i(\bar{y}_i, q) - \sum_{j \neq i} \beta_{ij}(\bar{p}_i - \bar{p}_j, q)_{\mathcal{Q}} = \langle g_i, q \rangle$$

for $i = 1, \dots, m$ and all test functions $v \in \mathcal{V}$, $z \in \mathcal{Z}$, and $q \in \mathcal{Q}$. Here, we need m history functions for $\bar{p}_i|_{[-\tau, 0]}(t) = \Phi_i(t)$ and set

$$(4.3) \quad \Phi_i(-\tau) = \Phi_i(0) = p_i^0, \quad \Phi_i \in C^\infty([-\tau, 0], \mathcal{Q}).$$

This then implies $\bar{p}_i(0) = p_i(0)$ and $\bar{u}(0) = u(0)$. As for the two-field formulation, we compare the solutions of the original and the delay system.

Proposition 4.1. *Assume sufficiently smooth right-hand sides f , g_i and history functions Φ_i as defined in (4.3) such that the solution of (4.2) satisfies $\bar{p}_i \in W^{2,\infty}(\mathcal{Q})$ for all $i = 1, \dots, m$. Then, the difference of the solutions to (2.4) and (4.2) satisfy the estimate*

$$\|\bar{u}(t) - u(t)\|_{\mathcal{V}}^2 + \sum_{i=1}^m \|\bar{p}_i(t) - p_i(t)\|_{\mathcal{Q}}^2 + \sum_{i=1}^m \|\bar{y}_i - y_i\|_{L^2(\mathcal{H}_z)}^2 \lesssim \tau^2 m (1 + e^{C(1+4m^2\beta^2)t}) \bar{P}$$

with a constant C independent of τ and

$$\bar{P} := \sum_{i=1}^m \|\dot{\bar{p}}_i\|_{L^2(\mathcal{Q})}^2 + (1 + \tau^2) T \sum_{i=1}^m \left(\|\ddot{\Phi}_i\|_{L^\infty(-\tau, 0; \mathcal{Q})}^2 + \|\ddot{\bar{p}}_i\|_{L^\infty(\mathcal{Q})}^2 \right).$$

Proof. We introduce the error terms $e_u := \bar{u} - u$, $e_{y_i} := \bar{y}_i - y_i$, $e_{p_i} := \bar{p}_i - p_i$ and note that $e_u(0) = 0$ and $e_{p_i}(0) = 0$ by construction of the delay system (4.2). Using a Taylor expansion as in (3.4) for each p_i with some $\zeta_{i,t}, \xi_{i,t} \in (t - \tau, t) \subseteq (-\tau, T]$, we obtain the system

$$(4.4a) \quad a(e_u, v) - \sum_{i=1}^m d_i(v, e_{p_i}) = -\tau \sum_{i=1}^m d_i(v, \dot{\bar{p}}_i) + \frac{1}{2} \tau^2 \sum_{i=1}^m d_i(v, \ddot{\bar{p}}_i(\zeta_{i,t})),$$

$$(4.4b) \quad (e_{y_i}, z)_{\mathcal{H}_z} - \hat{d}_i(z, e_{p_i}) = 0,$$

$$(4.4c) \quad d_i(\dot{e}_u, q) + c(\dot{e}_{p_i}, q) + \hat{d}_i(e_{y_i}, q) = \sum_{j \neq i} \beta_{ij}(e_{p_i} - e_{p_j}, q)_{\mathcal{Q}}$$

for test functions $v \in \mathcal{V}$, $z \in \mathcal{Z}$, and $q \in \mathcal{Q}$. From equation (4.4b) and $e_{p_i}(0) = 0$ we conclude that also $e_{y_i}(0) = 0$ for all $i = 1, \dots, m$. Considering the derivatives of the first two equations, we get

$$(4.5a) \quad a(\dot{e}_u, v) - \sum_{i=1}^m d_i(v, \dot{e}_{p_i}) = -\tau \sum_{i=1}^m d_i(v, \ddot{\bar{p}}_i(\xi_{i,t})),$$

$$(4.5b) \quad (\dot{e}_{y_i}, z)_{\mathcal{H}_z} - \hat{d}_i(z, \dot{e}_{p_i}) = 0.$$

The sum of (4.5a) with $v = \dot{e}_u$, (4.5b) with $z = e_{y_i}$, and (4.4c) with $q = \dot{e}_{p_i}$ for all $i = 1, \dots, m$ leads to

$$\|\dot{e}_u\|_{\mathcal{V}}^2 + \sum_{i=1}^m \|\dot{e}_{p_i}\|_{\mathcal{Q}}^2 + \frac{d}{dt} \sum_{i=1}^m \|e_{y_i}\|_{\mathcal{H}_z}^2 \lesssim m \beta^2 \sum_{i=1}^m \sum_{j \neq i} \|e_{p_i} - e_{p_j}\|_{\mathcal{Q}}^2 + m \tau^2 \sum_{i=1}^m \|\ddot{p}_i(\xi_{i,t})\|_{\mathcal{Q}}^2.$$

Integration over $[0, t]$ then yields

$$\int_0^t \|\dot{e}_u(s)\|_{\mathcal{V}}^2 ds \lesssim m \beta^2 \sum_{i=1}^m \sum_{j \neq i} \int_0^t \|e_{p_i}(s) - e_{p_j}(s)\|_{\mathcal{Q}}^2 ds + m \tau^2 t \sum_{i=1}^m \|\ddot{p}_i\|_{L^\infty(-\tau, t; \mathcal{Q})}^2.$$

On the other hand, the sum of (4.4a) with $v = \dot{e}_u$, (4.4b) with $z = e_{y_i}$, and (4.4c) with $q = e_{p_i}$ for all $i = 1, \dots, m$ gives

$$\begin{aligned} & \frac{1}{2} \frac{d}{dt} \|e_u\|_{\mathcal{V}}^2 + \frac{1}{2} \frac{d}{dt} \sum_{i=1}^m \|e_{p_i}\|_{\mathcal{Q}}^2 + \sum_{i=1}^m \|e_{y_i}\|_{\mathcal{H}_z}^2 \\ & \lesssim m \beta^2 \sum_{i=1}^m \sum_{j \neq i} \|e_{p_i} - e_{p_j}\|_{\mathcal{Q}}^2 + \sum_{i=1}^m \|e_{p_i}\|_{\mathcal{Q}}^2 + \|\dot{e}_u\|_{\mathcal{V}}^2 + m \tau^2 \sum_{i=1}^m \|\dot{p}_i\|_{\mathcal{Q}}^2 + m \tau^4 \sum_{i=1}^m \|\ddot{p}_i(\zeta_{i,t})\|_{\mathcal{Q}}^2. \end{aligned}$$

We integrate again over $[0, t]$ and use the previous estimate of the integral of $\|\dot{e}_u\|_{\mathcal{V}}^2$. With the triangle inequality applied to $\|e_{p_i}(s) - e_{p_j}(s)\|_{\mathcal{Q}}^2$ this then yields

$$\begin{aligned} & \|e_u(t)\|_{\mathcal{V}}^2 + \sum_{i=1}^m \|e_{p_i}(t)\|_{\mathcal{Q}}^2 + \sum_{i=1}^m \int_0^t \|e_{y_i}(s)\|_{\mathcal{H}_z}^2 ds \\ & \lesssim (1 + 4m^2 \beta^2) \sum_{i=1}^m \int_0^t \|e_{p_i}(s)\|_{\mathcal{Q}}^2 ds + m \tau^2 \sum_{i=1}^m \|\dot{p}_i\|_{L^2(0, t; \mathcal{Q})}^2 + m (\tau^2 + \tau^4) t \sum_{i=1}^m \|\ddot{p}_i\|_{L^\infty(-\tau, t; \mathcal{Q})}^2. \end{aligned}$$

Finally, an application of Grönwall's inequality provides

$$\sum_{i=1}^m \|e_{p_i}(t)\|_{\mathcal{Q}}^2 \leq C m e^{C(1+4m^2\beta^2)t} \left[\tau^2 \sum_{i=1}^m \|\dot{p}_i\|_{L^2(0, t; \mathcal{Q})}^2 + (\tau^2 + \tau^4) t \sum_{i=1}^m \|\ddot{p}_i\|_{L^\infty(-\tau, t; \mathcal{Q})}^2 \right],$$

where C is the constant hidden in \lesssim of the previous estimate. Note that this constant is independent of the discretization parameter τ . \square

The latter result shows that the solutions of the original network model (2.4) and the corresponding delay model (4.2) only differ by a term of order τ as long as $\bar{P}(t)$ stays bounded, i.e., as long as the delay system has a stable solution. Recall that this stability issue is discussed in Appendix A for the two-field model. In the setting of smooth data and regular solutions considered there, the two- and three-field formulation are equivalent. In the network case, the operators turn into operator matrices with similar properties. The only difference is that the ellipticity of the differential operator becomes a Gårding inequality. This, however, does not effect the stability result.

We move on with the discretization of the delay system, which defines the semi-explicit scheme introduced in (4.1).

4.2. Spatial projection. Let $u \in \mathcal{V}$, $y_i \in \mathcal{Z}$, and $p_i \in \mathcal{Q}$, $i = 1, \dots, m$. Based on the network system (2.4) and the discrete spaces V_h , Z_h , and Q_h , we define two projection operators. As in the two-field model we define $R_u: \mathcal{V} \rightarrow V_h$ by

$$(4.6) \quad a(R_u u, v_h) = a(u, v_h)$$

for all $v_h \in V_h$. Note that this problem is uniquely solvable due to the ellipticity of a . Second, we define the coupled projection $R_i: \mathcal{Z} \times \mathcal{Q} \rightarrow Z_h \times Q_h$ and write in short $R_i y_i$ and $R_i p_i$ for the parts of $R_i(y_i, p_i)$ in Z_h and Q_h , respectively. Using this notation, we define

$$(4.7a) \quad (R_i y_i, z_h)_{\mathcal{H}_z} - \hat{d}_i(z_h, R_i p_i) = (y_i, z_h)_{\mathcal{H}_z} - \hat{d}_i(z_h, p_i),$$

$$(4.7b) \quad -\hat{d}_i(R_i y_i, q_h) = -\hat{d}_i(y_i, q_h)$$

for all $z_h \in Z_h$ and $q_h \in Q_h$. Due to the saddle point structure of (4.7), the system is uniquely solvable if the discrete inf-sup condition

$$\inf_{q_h \in Q_h} \sup_{z_h \in Z_h} \frac{\hat{d}_i(z_h, q_h)}{\|z_h\|_{\mathcal{Z}} \|q_h\|_{\mathcal{Q}}} \geq \gamma > 0$$

is fulfilled for each $i = 1, \dots, m$ and $(\cdot, \cdot)_{\mathcal{H}_z}$ is elliptic on the kernel of \hat{d}_i , see e.g. [BBF13, Ch. 4.2]. In the subsequent error analysis, we will assume that (4.7) attains a unique solution and that the projections satisfy the following approximation properties.

Assumption 4.2 (Spatial projection, network case). Consider $u \in \mathcal{V}$, $y_i \in \mathcal{Z}$, $p_i \in \mathcal{Q}$ and assume that (4.7) is well-posed. We assume that the projection errors satisfy

$$(4.8a) \quad \|u - R_u u\|_{\mathcal{V}} \lesssim h \|\nabla^2 u\|_{\mathcal{H}_V},$$

$$(4.8b) \quad \|y_i - R_i y_i\|_{\mathcal{H}_z} \lesssim h \|\nabla y_i\|_{\mathcal{H}_z},$$

$$(4.8c) \quad \|p_i - R_i p_i\|_{\mathcal{Q}} \lesssim h (\|\nabla y_i\|_{\mathcal{H}_z} + \|\nabla p_i\|_{\mathcal{Q}}),$$

if the derivatives $\nabla^2 u$, ∇y_i , and ∇p_i are bounded in \mathcal{H}_V , \mathcal{H}_z , and \mathcal{Q} , respectively.

Example 4.3. For the spaces $\mathcal{V} = [H_0^1(\Omega)]^d$, $\mathcal{H}_V = [L^2(\Omega)]^d$, $\mathcal{Z} = H_0(\text{div}, \Omega)$, $\mathcal{H}_z = [L^2(\Omega)]^d$, and $\mathcal{Q} = L^2(\Omega)$, Assumption 4.2 is satisfied if V_h equals the P_1 Lagrange finite element space, Z_h the Raviart-Thomas space RT_0 , and Q_h the piecewise constant P_0 space. For the proofs we refer to [Bra07, Ch. II.7] and [Dur08, Th. 3.3].

4.3. Full discretization of the delay system. As for the two-field model in Section 3, we now analyze the implicit time discretization of the delay PDAE (4.2), since this is equal to the proposed semi-explicit scheme (4.1).

Proposition 4.4. Suppose Assumptions 2.6, 2.7, and 4.2 and the assumptions of Proposition 4.1 hold, as well as $\nabla^2 \bar{u} \in L^\infty(\mathcal{H}_V)$, $\nabla \bar{y}_i \in W^{1,\infty}(\mathcal{H}_z)$, and $\nabla \bar{p}_i \in W^{1,\infty}(\mathcal{Q})$. Then, taking initial data $u_h^0 \in V_h$ and $p_{i,h}^0 \in Q_h$ with

$$\|R_u u^0 - u_h^0\|_{\mathcal{V}} + \sum_{i=1}^m \|R_i p_i^0 - p_{i,h}^0\|_{\mathcal{Q}} \lesssim h$$

implies that for all $n \leq T/\tau$ the solution of the fully discretized system (4.1) satisfies

$$\|\bar{u}(t_n) - u_h^n\|_{\mathcal{V}}^2 + \sum_{i=1}^m \|\bar{p}_i(t_n) - p_{i,h}^n\|_{\mathcal{Q}}^2 + \sum_{k=1}^n \sum_{i=1}^m \tau \|\bar{y}_i(t_k) - y_{i,h}^k\|_{\mathcal{H}_z}^2 \lesssim e^{2t_n} (1 + t_n) (h^2 + \tau^2).$$

Proof. We follow the same approach as in the proof of Proposition 3.6. First, we introduce

$$\eta_u^n := R_u \bar{u}^n - u_h^n \in V_h, \quad \eta_{y_i}^n := R_i \bar{y}_i^n - y_{i,h}^n \in Z_h, \quad \eta_{p_i}^n := R_i \bar{p}_i^n - p_{i,h}^n \in Q_h,$$

where $\bar{u}^n = \bar{u}(t_n)$, $\bar{y}_i^n = \bar{y}_i(t_n)$, and $\bar{p}_i^n = \bar{p}_i(t_n)$ are the solutions of (4.2) and R_u , R_i denote the projections defined in (4.6) and (4.7), respectively. With (4.1a) and (4.2a), we compute

$$a(\eta_u^{n+1}, v_h) - \sum_{i=1}^m d_i(v_h, \eta_{p_i}^{n+1}) = \sum_{i=1}^m \left[d_i(v_h, \bar{p}_i^n - R_i \bar{p}_i^n) - d_i(v_h, \eta_{p_i}^{n+1} - \eta_{p_i}^n) \right]$$

for all $v_h \in V_h$. Similarly, we obtain from (4.1b) and (4.2b) that

$$(\eta_{y_i}^{n+1}, z_h)_{\mathcal{H}_Z} - \hat{d}_i(z_h, \eta_{p_i}^{n+1}) = 0$$

for all $z_h \in Z_h$ and $i = 1, \dots, m$. Equations (4.1c) and (4.2c) yield

$$\begin{aligned} \tau \hat{d}_i(\eta_{y_i}^{n+1}, q_h) &= \tau \hat{d}_i(\bar{y}_i^{n+1}, q_h) - \tau \hat{d}_i(y_{i,h}^{n+1}, q_h) \\ &= -d_i(\tau \dot{\bar{u}}^{n+1}, q_h) - c(\tau \dot{\bar{p}}_i^{n+1}, q_h) + d_i(\tau D_\tau u_h^{n+1}, q_h) + c(\tau D_\tau p_{i,h}^{n+1}, q_h) \\ &\quad + \tau \sum_{j \neq i} \beta_{ij} ((\bar{p}_i^{n+1} - R_i \bar{p}_i^{n+1} + \eta_{p_i}^{n+1}) - (\bar{p}_j^{n+1} - R_j \bar{p}_j^{n+1} + \eta_{p_j}^{n+1}), q_h)_{\mathcal{Q}} \end{aligned}$$

for all $q_h \in Q_h$. Defining

$$\theta_u^{n+1} := R_u \bar{u}^{n+1} - R_u \bar{u}^n - \tau \dot{\bar{u}}^{n+1} \quad \text{and} \quad \theta_{p_i}^{n+1} := R_i \bar{p}_i^{n+1} - R_i \bar{p}_i^n - \tau \dot{\bar{p}}_i^{n+1},$$

we get with the particular test functions $v_h = \eta_u^{n+1} - \eta_u^n$, $z_h = \eta_{y_i}^{n+1}$, and $q_h = \eta_{p_i}^{n+1}$,

$$\begin{aligned} &a(\eta_u^{n+1}, \eta_u^{n+1} - \eta_u^n) + \sum_{i=1}^m c(\eta_{p_i}^{n+1} - \eta_{p_i}^n, \eta_{p_i}^{n+1}) + \tau \sum_{i=1}^m \|\eta_{y_i}^{n+1}\|_{\mathcal{H}_Z}^2 \\ &= \sum_{i=1}^m \left[d_i(\eta_u^{n+1} - \eta_u^n, \bar{p}_i^n - R_i \bar{p}_i^n - \tau D_\tau \eta_{p_i}^{n+1}) + d_i(\theta_u^{n+1}, \eta_{p_i}^{n+1}) + c(\theta_{p_i}^{n+1}, \eta_{p_i}^{n+1}) \right] \\ &\quad + \tau \sum_{i=1}^m \sum_{j \neq i} \beta_{ij} \left[(\bar{p}_i^{n+1} - R_i \bar{p}_i^{n+1} + \eta_{p_i}^{n+1}, \eta_{p_i}^{n+1})_{\mathcal{Q}} - (\bar{p}_j^{n+1} - R_j \bar{p}_j^{n+1} + \eta_{p_j}^{n+1}, \eta_{p_i}^{n+1})_{\mathcal{Q}} \right]. \end{aligned}$$

Using Lemma 3.7 for the bilinear forms a and c , we obtain

$$\begin{aligned} &\|\eta_u^{n+1}\|_a^2 - \|\eta_u^n\|_a^2 + \|\tau D_\tau \eta_u^{n+1}\|_a^2 + \sum_{i=1}^m \left[\|\eta_{p_i}^{n+1}\|_c^2 - \|\eta_{p_i}^n\|_c^2 + \|\tau D_\tau \eta_{p_i}^{n+1}\|_c^2 + 2\tau \|\eta_{y_i}^{n+1}\|_{\mathcal{H}_Z}^2 \right] \\ &= 2 \sum_{i=1}^m \left[d_i(\tau D_\tau \eta_u^{n+1}, \bar{p}_i^n - R_i \bar{p}_i^n - \tau D_\tau \eta_{p_i}^{n+1}) + d_i(\theta_u^{n+1}, \eta_{p_i}^{n+1}) + c(\theta_{p_i}^{n+1}, \eta_{p_i}^{n+1}) \right] \\ &\quad + 2\tau \sum_{i=1}^m \sum_{j \neq i} \beta_{ij} \left[(\bar{p}_i^{n+1} - R_i \bar{p}_i^{n+1} + \eta_{p_i}^{n+1}, \eta_{p_i}^{n+1})_{\mathcal{Q}} - (\bar{p}_j^{n+1} - R_j \bar{p}_j^{n+1} + \eta_{p_j}^{n+1}, \eta_{p_i}^{n+1})_{\mathcal{Q}} \right]. \end{aligned}$$

Rewriting the first term on the right-hand side as for the two-field model and using the Taylor expansion for \bar{p}_i^n , we can estimate

$$2 d_i(\tau D_\tau \eta_u^{n+1}, \bar{p}_i^n - R_i \bar{p}_i^n - \tau D_\tau \eta_{p_i}^{n+1})$$

$$\begin{aligned} &\leq \frac{C_{d_i}^2}{c_a c_c} \|\tau D_\tau \eta_u^{n+1}\|_a^2 + \|\tau D_\tau \eta_{p_i}^{n+1}\|_c^2 + \frac{\tau}{m} \|\eta_u^n\|_a^2 + \tau \frac{m C_{d_i}^2}{c_a} \|\dot{p}_i - R_i \dot{p}_i\|_{L^\infty(\mathcal{Q})}^2 \\ &\quad + 2 d_i(\eta_u^{n+1}, \bar{p}_i^n - R_i \bar{p}_i^n) - 2 d_i(\eta_u^n, \bar{p}_i^{n-1} - R_i \bar{p}_i^{n-1}). \end{aligned}$$

Further, we have the two estimates

$$d_i(\theta_u^{n+1}, \eta_{p_i}^{n+1}) \leq \frac{C_{d_i}^2}{c_c} \frac{1}{\tau} \|\theta_u^{n+1}\|_{\mathcal{V}}^2 + \frac{\tau}{4} \|\eta_{p_i}^{n+1}\|_c^2, \quad c(\theta_{p_i}^{n+1}, \eta_{p_i}^{n+1}) \leq \frac{C_c^2}{\tau} \|\theta_{p_i}^{n+1}\|_{\mathcal{Q}}^2 + \frac{\tau}{4} \|\eta_{p_i}^{n+1}\|_c^2,$$

and the double sum including the exchange rates β_{ij} is bounded from above by

$$2\tau\beta(m-1) \sum_{i=1}^m \left[\|\bar{p}_i^{n+1} - R_i \bar{p}_i^{n+1}\|_{\mathcal{Q}}^2 + \frac{3}{c_c} \|\eta_{p_i}^{n+1}\|_c^2 \right].$$

We combine the previous estimates and absorb the terms $\|\tau D_\tau \eta_{p_i}^{n+1}\|_c^2$ and $\|\tau D_\tau \eta_u^{n+1}\|_a^2$ using Assumption 2.6 for the latter. Further, we apply $6\beta(m-1) \leq c_c$ from Assumption 2.7. This yields

$$\begin{aligned} &\|\eta_u^{n+1}\|_a^2 - (1 + \tau) \|\eta_u^n\|_a^2 + \sum_{i=1}^m \left[(1 - 2\tau) \|\eta_{p_i}^{n+1}\|_c^2 - \|\eta_{p_i}^n\|_c^2 + 2\tau \|\eta_{y_i}^{n+1}\|_{\mathcal{H}_z}^2 \right] \\ &\quad - 2 \sum_{i=1}^m d_i(\eta_u^{n+1}, \bar{p}_i^n - R_i \bar{p}_i^n) + 2 \sum_{i=1}^m d_i(\eta_u^n, \bar{p}_i^{n-1} - R_i \bar{p}_i^{n-1}) \\ &\lesssim \sum_{i=1}^m \left[\tau m \|\dot{p}_i - R_i \dot{p}_i\|_{L^\infty(\mathcal{Q})}^2 + 2\tau\beta(m-1) \|\bar{p}_i^{n+1} - R_i \bar{p}_i^{n+1}\|_{\mathcal{Q}}^2 + \frac{1}{\tau} \|\theta_u^{n+1}\|_{\mathcal{V}}^2 + \frac{1}{\tau} \|\theta_{p_i}^{n+1}\|_{\mathcal{Q}}^2 \right]. \end{aligned}$$

As in the proof of Proposition 3.6 we can apply Assumption 4.2 to bound θ_u^{n+1} and $\theta_{p_i}^{n+1}$, leading to

$$\begin{aligned} \|\theta_u^{n+1}\|_{\mathcal{V}} &\lesssim \tau h \|\nabla^2 \dot{u}\|_{L^\infty(\mathcal{H}_v)} + \tau^2 \|\ddot{u}\|_{L^\infty(\mathcal{V})}, \\ \|\theta_{p_i}^{n+1}\|_{\mathcal{Q}} &\lesssim \tau h \|\nabla \dot{y}_i\|_{L^\infty(\mathcal{H}_z)} + \tau h \|\nabla \dot{p}_i\|_{L^\infty(\mathcal{Q})} + \tau^2 \|\ddot{p}_i\|_{L^\infty(\mathcal{Q})}. \end{aligned}$$

Finally, the discrete version of the Grönwall lemma gives

$$\|\eta_u^n\|_{\mathcal{V}}^2 + \sum_{i=1}^m \|\eta_{p_i}^n\|_{\mathcal{Q}}^2 + \sum_{k=1}^n \sum_{i=1}^m \tau \|\eta_{y_i}^k\|_{\mathcal{H}_z}^2 \lesssim e^{2t_n} (1 + t_n) (h^2 + \tau^2)$$

such that the assertion follows by Assumption 4.2 and the triangle inequality. \square

4.4. Convergence of the semi-explicit scheme. The combination of Propositions 4.1 and 4.4 provides the desired convergence property of the semi-explicit scheme (4.1).

Theorem 4.5 (Convergence, network model). *Suppose Assumptions 2.6, 2.7, and 4.2 hold. Further, let the right-hand sides $f: [0, T] \rightarrow \mathcal{H}_v$ and $g_i: [0, T] \rightarrow \mathcal{Q}$ be sufficiently smooth. Then, with (u, y_i, p_i) being the solution of the original system (2.4) and $u_h^n \in V_h$, $y_{i,h}^n \in Z_h$, $p_{i,h}^n \in Q_h$ the fully discrete approximations obtained by (4.1) for $n \leq T/\tau$ and initial data $u_h^0 \in V_h$, $p_{i,h}^0 \in Q_h$ with*

$$\|R_u u^0 - u_h^0\|_{\mathcal{V}} + \sum_{i=1}^m \|R_i p_i^0 - p_{i,h}^0\|_{\mathcal{Q}} \lesssim h$$

we obtain the error estimate

$$\|u(t_n) - u_h^n\|_{\mathcal{V}}^2 + \sum_{i=1}^m \|p_i(t_n) - p_{i,h}^n\|_{\mathcal{Q}}^2 + \sum_{k=1}^n \sum_{i=1}^m \tau \|y_i(t_k) - y_{i,h}^k\|_{\mathcal{H}_z}^2 \lesssim e^{Ct_n} (1 + t_n) (h^2 + \tau^2)$$

with a constant C depending on β , but independent of τ and h .

Proof. We define the history functions Φ_i as in (4.3). As in the two-field case, the assumptions on the data and the assumed H^2 -regularity imply that the solution of the related delay system (4.2) stays bounded. Thus, following the procedure presented in Appendix A, we conclude $\nabla^2 \bar{u} \in L^\infty(\mathcal{H}_v)$, $y_i, \bar{y}_i \in W^{2,\infty}(\mathcal{H}_z)$, $\nabla \bar{y}_i \in W^{1,\infty}(\mathcal{H}_z)$, $\bar{p}_i \in W^{2,\infty}(\mathcal{Q})$, and $\nabla \bar{p}_i \in W^{1,\infty}(\mathcal{Q})$. With this, all assumptions of Propositions 4.1 and 4.4 are satisfied and the stated estimate follows from the previous results and the triangle inequality. Note that the estimate of the y_i -terms requires an application of the trapezoidal rule for the function $\sum_{i=1}^m \|\bar{y}_i(t) - y_i(t)\|_{\mathcal{H}_z}^2$. \square

5. NUMERICAL EXAMPLES

This section is devoted to the numerical illustration of the convergence results presented in Theorems 3.9 and 4.5 and corresponding runtime comparisons. Furthermore, we show that the weak coupling condition is sharp and actually a necessary condition for the convergence of the semi-explicit scheme.

All computations use a FEniCS finite element implementation and have been performed on an HPC Infiniband cluster.

5.1. Linear poroelasticity. We test the semi-explicit time-integration with the linear poroelasticity example presented in Example 2.2. The parameters for the simulation (omitting the units) are given by

$$\begin{array}{ccccc} \lambda & \mu & \frac{\kappa}{\nu} & \frac{1}{M} & \alpha \\ \hline 1.2 \times 10^{10} & 6.0 \times 10^9 & 6.33 \times 10^2 & 7.8 \times 10^3 & 0.79 \end{array}.$$

The simulation is performed in the two-dimensional unit square $\Omega = (0, 1)^2$ with final time $T = 10$. The source terms and the initial condition are chosen as

$$f \equiv 0, \quad g(t) = 10 e^t, \quad \text{and} \quad p^0(x, y) = 3000 x(1 - x) y(1 - y).$$

For the error analysis, we compute a reference solution with mesh size $h = 1.95 \times 10^{-3}$ (with standard P_1 finite elements and homogeneous Dirichlet boundary conditions, cf. Example 3.5) and time step size $\tau = 4.88 \times 10^{-3}$. The relative errors in the energy norms $\|\cdot\|_a$ and $\|\cdot\|_c$ at the final time are depicted in Figure 5.1.

For the pressure variable (right plot in Figure 5.1), we observe a linear decay of the error with respect to the time step size in agreement with Theorem 3.9. The relative error in the displacement (left plot in Figure 5.1) is dominated by the spatial discretization error, which also shows the predicted linear decay. Thus, the numerical experiment confirms our theoretical findings. It is worth to mention that the semi-explicit Euler performs very similarly as the implicit Euler with a negligible difference.

5.2. A network example. We consider a simple network example with $m = 4$, i.e., we have four pressure variables. The used parameters are mainly motivated by the ones considered in [VCT⁺16, JCLT19] and given by

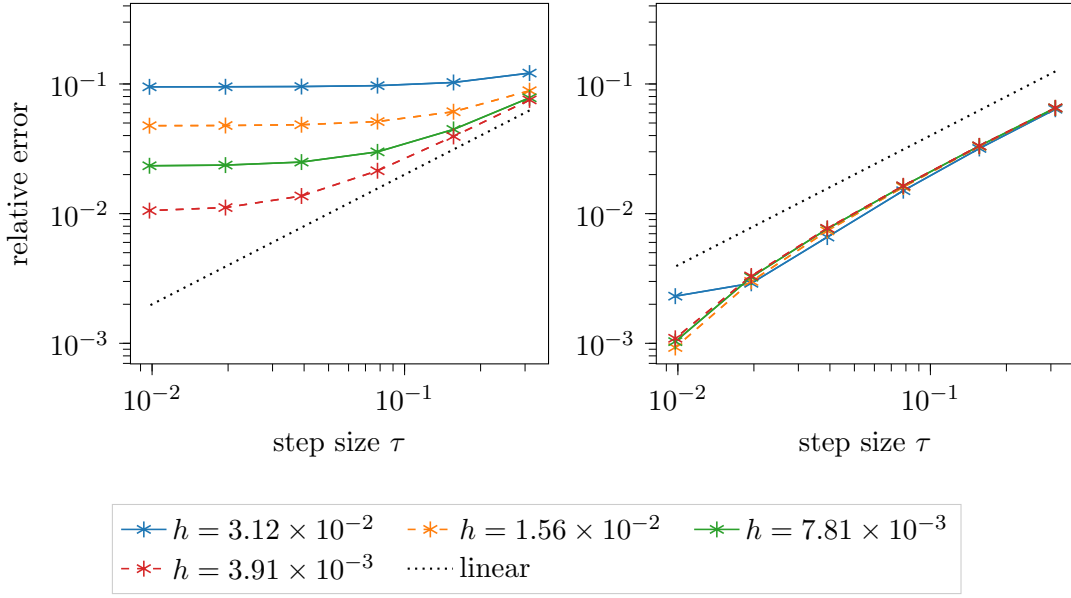


FIGURE 5.1. Relative error at final time $T = 10$ for the implicit (stars) and the semi-explicit Euler scheme (solid/dashed line) for different mesh sizes h . Left: displacement u . Right: pressure p .

$$\begin{array}{ccccccccc} \lambda & \mu & \frac{\kappa_1}{\nu_1} = \frac{\kappa_2}{\nu_2} & \frac{\kappa_3}{\nu_3} & \frac{\kappa_4}{\nu_5} & \frac{1}{M} & \alpha_i \\ \hline 7786.42 & 3337.037 & 3.75 \times 10^{-4} & 1.57 \times 10^{-5} & 3.75 \times 10^{-5} & 4.50 \times 10^{-2} & 0.99 \end{array}.$$

Further, the parameters β_{ij} , $i, j \in \{1, 2, 3, 4\}$ are set to zero, besides

$$\beta_{12} = \beta_{24} = 1.5 \times 10^{-19}, \quad \beta_{23} = 2 \times 10^{-19}, \quad \beta_{34} = 1 \times 10^{-13}.$$

The simulation is performed in the domain $\Omega = (0, 1)^2 \setminus B_{0.25}((0.5, 0.5))$ with $T = 10$ and using the P_1 finite element space for the displacement, the Raviart-Thomas space of lowest order RT_0 for the fluid fluxes, and the space P_0 of piecewise constants for the pressures. The source terms are given by $f \equiv 0$ and $g \equiv 0$ and the initial pressures are chosen as $p_2^0 \equiv p_4^0 \equiv 650$, $p_3^0 \equiv 1000$ and

$$p_1^0(x, y) = \mathbb{1}_{\Omega_p}(13300 - 3238400((x - 0.75)^2 + (y - 0.75)^2)) + \mathbb{1}_{\Omega \setminus \Omega_p} 650$$

with $\Omega_p = \{(x, y) \in \Omega : (x - 0.75)^2 + (y - 0.75)^2 \leq 1/256\}$. This means that three initial pressures are constant and p_1^0 has a local peak.

As predicted by Theorem 4.5, we have linear convergence in time and space, very similar to the previous example. The respective runtimes for the implicit and semi-explicit schemes are given in Table 5.1. The numbers show that a significant percentage of the computation time can be saved when computing with the semi-explicit scheme. This is of particular value for small mesh and step sizes h and τ . Further note that we did not yet exploit the fact that the decoupled nature of the semi-explicit method facilitates the use of preconditioned iterative methods.

The displacement and the pressures at final time $T = 10$ for the choice $h = \tau = 2^{-7}$ are shown in Figure 5.2. One can observe that the high pressure peak in the pressure variable p_1 in the initial condition starts to average out across the whole domain and also

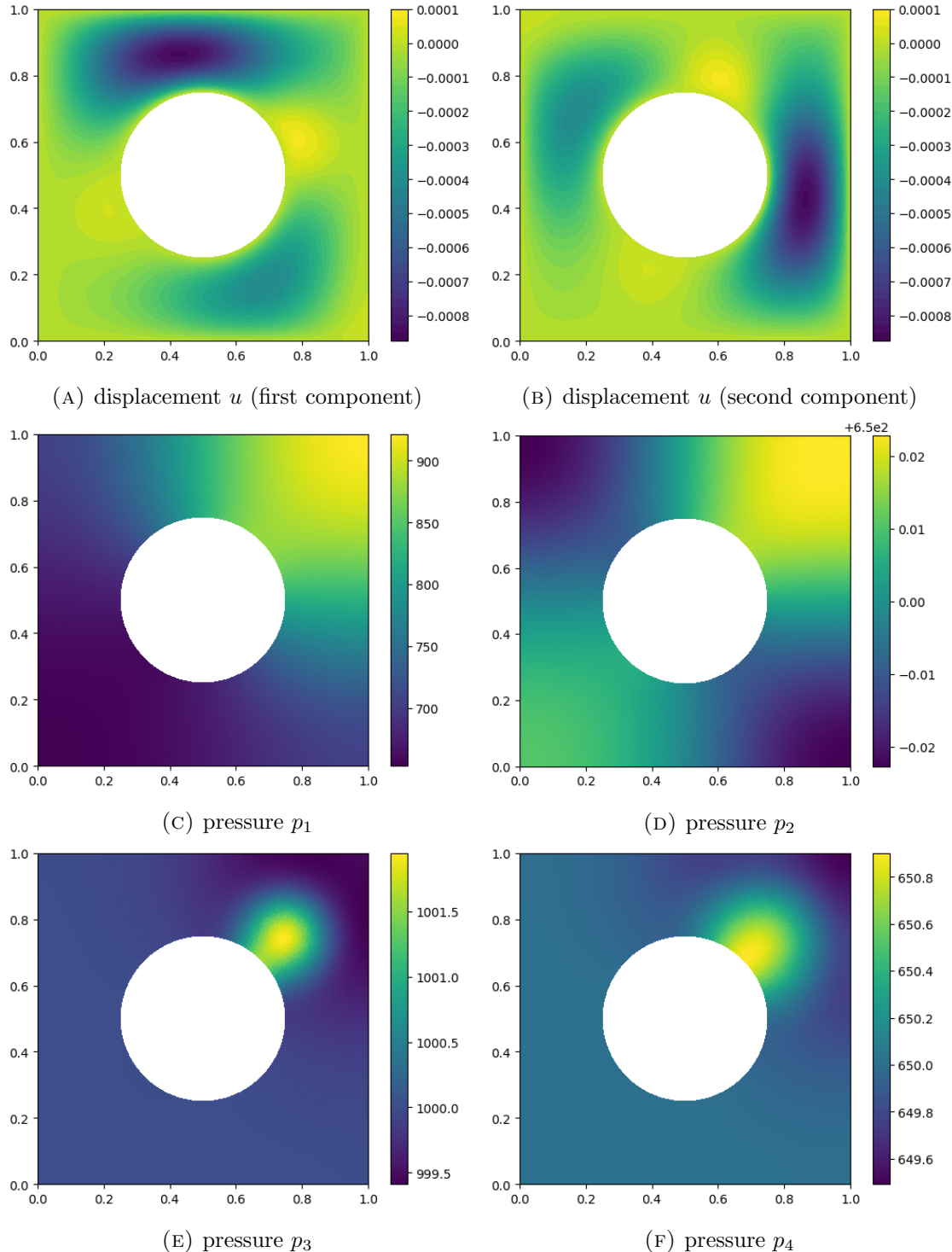


FIGURE 5.2. Displacement u and pressures p_i , $i \in \{1, 2, 3, 4\}$ at time $T = 10$ for the network case, computed with $h = \tau = 2^{-7}$.

TABLE 5.1. Runtime comparison (in seconds)

$h = \tau$	2^{-4}	2^{-5}	2^{-6}	2^{-7}	2^{-8}
implicit	13.2	65.8	471.0	4027.2	29921.1
semi-explicit	9.7	51.6	314.6	2544.2	19994.4
reduction (in %)	26.5	21.6	33.2	36.8	33.2

has an influence on the other pressure variables, especially on p_3 and p_4 where small local pressure increases can be observed. The effect on the pressure p_2 is only minor but not as local as for the pressures p_3 and p_4 . Moreover, the changes in the pressures also lead to a deformation of the object originating from the location of the original pressure peak.

5.3. Sharpness of the weak coupling condition. We conclude our numerical examples with an investigation of the weak coupling condition in Assumption 2.4. To this end, we consider a toy problem of the form (2.1) with $\mathcal{V} = \mathcal{H}_v = \mathbb{R}^3$, $\mathcal{Q} = \mathcal{H}_q = \mathbb{R}^1$ and bilinear forms

$$a(u, v) = v^T A u, \quad d(v, p) = \omega p^T D v, \quad c(p, q) = q^T C p, \quad b(p, q) = q^T B p$$

with matrices

$$A := \begin{bmatrix} 2 & -1 & 0 \\ -1 & 2 & -1 \\ 0 & -1 & 2 \end{bmatrix}, \quad D := \begin{bmatrix} 1 & 2 & 3 \end{bmatrix}, \quad C := 1, \quad \text{and} \quad B := 1.$$

The constants c_a and c_c are given by the smallest eigenvalue of A and C , respectively, i.e., $c_a \approx 0.586$ and $c_c = 1$. The continuity constant $C_d(\omega)$ is given by the spectral norm of ωD . In particular, we have $C_d(\omega) = |\omega| \|D\|_2 \approx 3.742 |\omega|$, i.e., the weak coupling condition from Assumption 2.4 requires $\omega \in [-0.2046, 0.2046]$. Moreover, in view of Example 3.3, the necessary and sufficient condition for the asymptotic stability of the related delay equation requires $\omega \in (-0.2182, 0.2182)$. We test our semi-explicit scheme with different step sizes τ and compute the relative error at the final time $T = 1$. For the forcing functions, we choose

$$f^T \equiv [1 \ 1 \ 1] \quad \text{and} \quad g(t) = \sin(t).$$

The results are presented in Figure 5.3, where the two critical values are represented with dashed lines. As expected from Theorem 3.9, the semi-explicit Euler schemes approximates the true solution well for all ω that satisfy the weak coupling condition. Independent of the step size τ we observe that the semi-explicit schemes fail when the related delay equation (3.2) becomes asymptotically unstable.

6. CONCLUSIONS

Within this paper, we have proven first-order convergence in time and space of the combination of the semi-explicit Euler scheme with a conforming finite element discretization. This result enables a more efficient time-stepping scheme as the linear system, which needs to be solved in every time step, decouples.

For the convergence analysis, we have employed a new technique which links the semi-explicit discretization to an implicit discretization of a related delay system. This approach

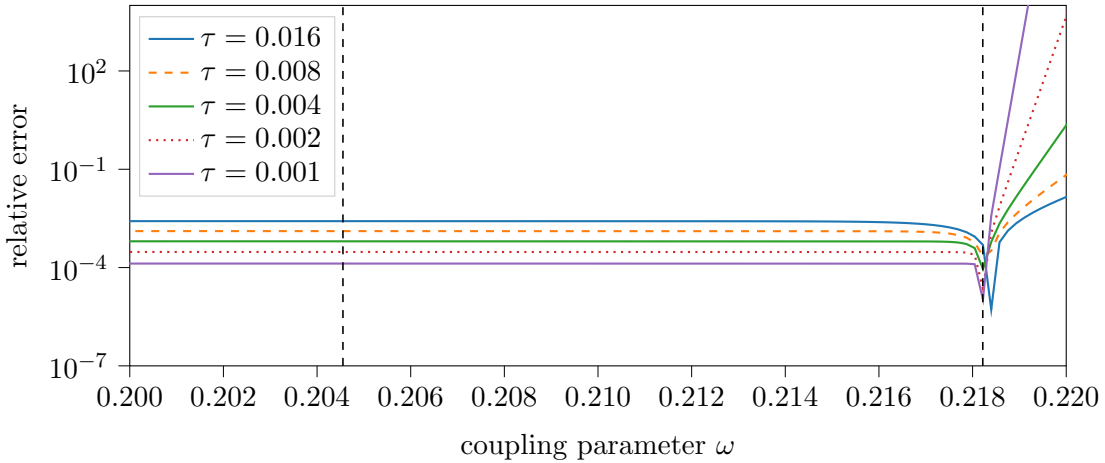


FIGURE 5.3. Relative error at the final time point $T = 1$ for different coupling parameters ω and different time step sizes τ .

also generates theoretical insight and explains the required weak coupling condition. Convergence of the method is proven for the classical two-field formulation (including poroelasticity) as well as for multiple-network systems which are of high interest in medical applications. The theoretical results are illustrated by three numerical experiments.

ACKNOWLEDGEMENTS

R. Maier gratefully acknowledges support by the German Research Foundation (DFG) in the Priority Program 1748 *Reliable simulation techniques in solid mechanics* (PE2143/2-2). The work of B. Unger is supported by the German Research Foundation (DFG) Collaborative Research Center 910 *Control of self-organizing nonlinear systems: Theoretical methods and concepts of application*, project number 163436311.

Major parts of the paper were evolved at CIRM in Luminy within a *Recherches en Binôme* (Research in Pairs) stay in August 2019. We are grateful for the invitation and kind hospitality. Further, we thank C. Carstensen (HU Berlin) for bringing up the idea of a semi-explicit discretization at CMAM-8 in Minsk.

REFERENCES

- [ACM⁺19] R. Altmann, E. Chung, R. Maier, D. Peterseim, and S.-M. Pun. Computational multiscale methods for linear heterogeneous poroelasticity. *J. Comput. Math.*, accepted for publication:1–18, 2019.
- [AH18] R. Altmann and J. Heiland. Regularization and Rothe discretization of semi-explicit operator DAEs. *Int. J. Numer. Anal. Model.*, 15(3):452–478, 2018.
- [Alt15] R. Altmann. *Regularization and Simulation of Constrained Partial Differential Equations*. Dissertation, Technische Universität Berlin, 2015.
- [AZ18] R. Altmann and C. Zimmer. On the smoothing property of linear delay partial differential equations. *J. Math. Anal. Appl.*, 467(2):916–934, 2018.
- [BBF13] D. Boffi, F. Brezzi, and M. Fortin. *Mixed finite element methods and applications*. Springer, Heidelberg, 2013.
- [BCP96] K.E. Brenan, S.L. Campbell, and L. R. Petzold. *Numerical solution of initial-value problems in differential-algebraic equations*. Society for Industrial and Applied Mathematics (SIAM), Philadelphia, PA, 1996.

- [BGZ99] A. Bellen, N. Guglielmi, and M. Zennaro. On the contractivity and asymptotic stability of systems of delay differential equations of neutral type. *BIT Numer. Math.*, 39(1):1–24, 1999.
- [Bio41] M. A. Biot. General theory of three-dimensional consolidation. *J. Appl. Phys.*, 12(2):155–164, 1941.
- [Bio56] M. A. Biot. Thermoelasticity and irreversible thermodynamics. *J. Appl. Phys.*, 27:240–253, 1956.
- [Bra07] D. Braess. *Finite Elements - Theory, Fast Solvers, and Applications in Solid Mechanics*. Cambridge University Press, New York, third edition, 2007.
- [BY11] Z. Z. Bai and X. Yang. On convergence conditions of waveform relaxation methods for linear differential-algebraic equations. *J. Comput. Appl. Math.*, 235(8):2790–2804, 2011.
- [BZ03] A. Bellen and M. Zennaro. *Numerical Methods for Delay Differential Equations*. Oxford University Press, New York, 2003.
- [Cam80] S. L. Campbell. Singular linear systems of differential equations with delays. *Appl. Anal.*, 11(2):129–136, 1980.
- [Cia88] P. G. Ciarlet. *Mathematical elasticity. Vol. I*. North-Holland, Amsterdam, 1988.
- [CR14] W. D. Callister and D. G. Rethwisch. *Materials science and engineering: An introduction*. Wiley, Hoboken, NJ, ninth edition, 2014.
- [DC93] E. Detournay and A. H. D. Cheng. Fundamentals of poroelasticity. In *Analysis and design methods*, pages 113–171. Elsevier, 1993.
- [Dur08] R. G. Durán. Mixed finite element methods. In *Mixed Finite Elements, Compatibility Conditions, and Applications*, pages 1–44. Springer, 2008.
- [EM09] A. Ern and S. Meunier. A posteriori error analysis of Euler-Galerkin approximations to coupled elliptic-parabolic problems. *ESAIM: Math. Model. Numer. Anal.*, 43(2):353–375, 2009.
- [EM13] E. Emmrich and V. Mehrmann. Operator differential-algebraic equations arising in fluid dynamics. *Comput. Methods Appl. Math.*, 13(4):443–470, 2013.
- [Eva98] L. C. Evans. *Partial Differential Equations*. American Mathematical Society (AMS), Providence, second edition, 1998.
- [FAC⁺19] S. Fu, R. Altmann, E. Chung, R. Maier, D. Peterseim, and S.-M. Pun. Computational multiscale methods for linear poroelasticity with high contrast. *J. Comput. Phys.*, 395:286–297, 2019.
- [Fu19] G. Fu. A high-order HDG method for the Biot’s consolidation model. *Comput. Math. Appl.*, 77(1):237–252, 2019.
- [GKC03] K. Gu, V. L. Kharitonov, and J. Chen. *Stability of Time-Delay Systems*. Birkhäuser, Boston, MA, 2003.
- [HK18] Q. Hong and J. Kraus. Parameter-robust stability of classical three-field formulation of Biot’s consolidation model. *Electron. Trans. Numer. Anal.*, 48:202–226, 2018.
- [HKLP19] Q. Hong, J. Kraus, M. Lymbery, and F. Philo. Conservative discretizations and parameter-robust preconditioners for Biot and multiple-network flux-based poroelasticity models. *Numer. Linear Algebr.*, 26(4):e2242, 2019.
- [HRGZ17] X. Hu, C. Rodrigo, F. J. Gaspar, and L. T. Zikatanov. A nonconforming finite element method for the Biot’s consolidation model in poroelasticity. *J. Comput. Appl. Math.*, 310:143–154, 2017.
- [JCLT19] G. Jv, M. Cai, J. Li, and J. Tian. Parameter-robust multiphysics algorithms for Biot model with application in brain edema simulation. ArXiv Preprint 1906.08802, 2019.
- [KM06] P. Kunkel and V. Mehrmann. *Differential-Algebraic Equations. Analysis and Numerical Solution*. European Mathematical Society, Zürich, 2006.
- [LMW17] J. J. Lee, K.-A. Mardal, and R. Winther. Parameter-robust discretization and preconditioning of Biot’s consolidation model. *SIAM J. Sci. Comput.*, 39(1):A1–A24, 2017.
- [Mie89] U. Miekkala. Dynamic iteration methods applied to linear DAE systems. *J. Comput. Appl. Math.*, 25:133–151, 1989.
- [MP17] A. Målqvist and A. Persson. A generalized finite element method for linear thermoelasticity. *ESAIM: Math. Model. Numer. Anal.*, 51(4):1145–1171, 2017.
- [PW07a] P. J. Phillips and M. F. Wheeler. A coupling of mixed and continuous Galerkin finite element methods for poroelasticity I: the continuous in time case. *Comput. Geosci.*, 11(2):131–144, 2007.

- [PW07b] P. J. Phillips and M. F. Wheeler. A coupling of mixed and continuous Galerkin finite element methods for poroelasticity II: the discrete-in-time case. *Comput. Geosci.*, 11(2):145–158, 2007.
- [PW08] P. J. Phillips and M. F. Wheeler. A coupling of mixed and discontinuous Galerkin finite-element methods for poroelasticity. *Comput. Geosci.*, 12(4):417–435, 2008.
- [RNM⁺03] T. Roose, P. A. Netti, L. L. Munn, Y. Boucher, and R. K. Jain. Solid stress generated by spheroid growth estimated using a linear poroelasticity model. *Microvasc. Res.*, 66(3):204–212, 2003.
- [Sho00] R. E. Showalter. Diffusion in poro-elastic media. *J. Math. Anal. Appl.*, 251(1):310–340, 2000.
- [Tar06] L. Tartar. *An Introduction to Navier-Stokes Equation and Oceanography*. Springer, Berlin, Heidelberg, 2006.
- [TU19] S. Trenn and B. Unger. Delay regularity of differential-algebraic equations. Preprint, submitted for publication, 2019.
- [TV11] B. Tully and Y. Ventikos. Cerebral water transport using multiple-network poroelastic theory: application to normal pressure hydrocephalus. *J. Fluid Mech.*, 667:188–215, 2011.
- [Ung18] B. Unger. Discontinuity propagation in delay differential-algebraic equations. *Electron. J. Linear Algebr.*, 34:582–601, 2018.
- [VCT⁺16] J. C. Vardakas, D. Chou, B. J. Tully, C. C. Hung, T. H. Lee, P. H. Tsui, and Y. Ventikos. Investigating cerebral oedema using poroelasticity. *Med. Eng. Phys.*, 38(1):48–57, 2016.
- [WG07] M. F. Wheeler and X. Gai. Iteratively coupled mixed and Galerkin finite element methods for poro-elasticity. *Numer. Meth. Part. D. E.*, 23(4):785–797, 2007.
- [Zei90] E. Zeidler. *Nonlinear Functional Analysis and its Applications IIa: Linear Monotone Operators*. Springer-Verlag, New York, 1990.
- [Zob10] M. D. Zoback. *Reservoir Geomechanics*. Cambridge University Press, Cambridge, 2010.

APPENDIX A. STABILITY OF THE DELAY EQUATION FOR THE TWO-FIELD MODEL

In order to prove Proposition 3.2, we need $\bar{p} \in W^{2,\infty}(\mathcal{H}_Q)$, where (\bar{u}, \bar{p}) is the solution of the delay PDAE (3.2). In the following we assume smooth data and show that this guarantees the existence of a solution and a uniform bounded in $W^{2,\infty}(\mathcal{H}_Q)$. We expect, however, that this result can be proven with weaker assumptions on the data, for instance, by extending the technique of [BGZ99] to the PDE setting. Since the main focus of this article is the convergence result for the semi-explicit scheme, we consider this future research.

For the stability analysis we consider a prototypical system of the form

- (A.1a) $\langle \dot{\bar{p}}(t) + \mathcal{K}\bar{p}(t), q \rangle = \langle \omega \dot{\bar{p}}(t - \tau) + \tilde{g}(t), q \rangle, \quad t \in (0, T],$
- (A.1b) $\bar{p}(t) = \Phi(t), \quad t \in [-\tau, 0]$

for all test functions $q \in \mathcal{Q}$ and with smooth history function $\Phi: [-\tau, 0] \rightarrow \mathcal{H}_Q$, source term $\tilde{g}: [0, T] \rightarrow \mathcal{Q}^*$, a constant $\omega \in \mathbb{R}$, and a linear, bounded operator $\mathcal{K}: \mathcal{Q} \rightarrow \mathcal{Q}^*$ that satisfies a Gårding inequality, i.e.,

$$(A.2) \quad \langle \mathcal{K}q, q \rangle \geq \kappa_{\mathcal{Q}} \|q\|_{\mathcal{Q}}^2 - \kappa_{\mathcal{H}_Q} \|q\|_{\mathcal{H}_Q}^2$$

for real constants $\kappa_{\mathcal{Q}} > 0$, $\kappa_{\mathcal{H}_Q} \geq 0$ and all $q \in \mathcal{Q}$.

Thus, we first need to reduce the delay PDAE (3.2) to such a parabolic problem with neutral delay. With the operators \mathcal{A} , \mathcal{B} , \mathcal{C} , \mathcal{D} corresponding to the bilinear forms a , b , c , d , respectively, system (3.2) can be written as

$$\mathcal{A}\bar{u} - \mathcal{D}^*\bar{p}(\cdot - \tau) = f \quad \text{in } \mathcal{V}^*, \quad \mathcal{D}\dot{\bar{u}} + \mathcal{C}\dot{\bar{p}} + \mathcal{B}\bar{p} = g \quad \text{in } \mathcal{Q}^*.$$

Since $\mathcal{A}: \mathcal{V} \rightarrow \mathcal{V}^*$ is an invertible operator, we can differentiate the first equation in time and insert it into the second equation. Using also the invertibility of \mathcal{C} , we get

$$\dot{\bar{p}} + \mathcal{C}^{-1}\mathcal{B}\bar{p} = \tilde{g} - \mathcal{C}^{-1}\mathcal{D}\mathcal{A}^{-1}\mathcal{D}^*\dot{\bar{p}}(\cdot - \tau)$$

with $\tilde{g} := \mathcal{C}^{-1}g - \mathcal{C}^{-1}\mathcal{D}\mathcal{A}^{-1}\dot{f}$. Considering d as bilinear form $d: \mathcal{V} \times \mathcal{H}_\omega \rightarrow \mathbb{R}$, we note that the operator $\mathcal{C}^{-1}\mathcal{D}\mathcal{A}^{-1}\mathcal{D}^*: \mathcal{H}_\omega \rightarrow \mathcal{H}_\omega$ is bounded with constant $\omega := C_d^2/(c_a c_c)$. For the stability analysis we can thus replace this operator by the constant ω .

We like to emphasize that the reduction from the PDAE (3.2) to the parabolic problem (A.1) comes along with the differentiation of the delay term. Although (3.2) seems to be of retarded type at first sight (only $\bar{p}(\cdot - \tau)$ appears), the reformulation shows that it is in fact *neutral*. This is due to the fact that the delay term appears in the elliptic equation and thus, in terms of DAEs, in the constraint.

Following [AZ18], we call a function $\bar{p} \in C([0, T]; \mathcal{H}_\omega) \cap L^2(\mathcal{Q})$ with $\dot{\bar{p}} \in L^2(\mathcal{Q}^*)$ a weak solution of (A.1), if $\bar{p}(0^+) = \bar{p}^0 \in \mathcal{H}_\omega$ and

$$\tilde{p}(t) := \begin{cases} \Phi(t), & t \in [-\tau, 0), \\ \bar{p}, & t \in [0, T] \end{cases}$$

satisfies (A.1) in the variational sense.

Proposition A.1. *Consider the initial trajectory problem (A.1) with $\tilde{g} \in L^2(\mathcal{Q}^*)$ and history function $\Phi \in C^1([-\tau, 0]; \mathcal{H}_\omega)$. If the bilinear form associated with \mathcal{K} satisfies a Gårding inequality (A.2), then (A.1) possesses a unique weak solution.*

Proof. On the interval $I_1 := [0, \tau]$ we have to solve the initial value problem

$$\begin{aligned} \dot{\bar{p}}_{I_1}(t) + \mathcal{K}\bar{p}_{I_1}(t) &= \tilde{g}(t) + \omega \dot{\Phi}(t - \tau), \\ \bar{p}_{I_1}(0) &= \Phi(0) \in \mathcal{H}_\omega. \end{aligned}$$

The assumptions imply $\tilde{g} + \omega \dot{\Phi}(\cdot - \tau) \in L^2(0, \tau, \mathcal{Q}^*)$ and thus the theorem of Lions-Tartar [Tar06, Lem. 19.1] guarantees a unique solution $\bar{p}_{I_1} \in C([0, \tau]; \mathcal{H}_\omega) \cap L^2(0, \tau; \mathcal{Q})$ with $\dot{\bar{p}}_{I_1} \in L^2(0, \tau; \mathcal{Q}^*)$. In particular, we conclude $\bar{p}_{I_1}(\tau) \in \mathcal{H}_\omega$. Applying Bellmann's method of steps (cf. [BZ03, Ch. 3.4]), we inductively infer that the sequence

$$\begin{aligned} \dot{\bar{p}}_{I_n} + \mathcal{K}\bar{p}_{I_n} &= \tilde{g}_{I_n} + \omega \dot{\bar{p}}_{I_{n-1}}, \\ \bar{p}_{I_n}(0) &= \bar{p}_{I_{n-1}}(\tau) \end{aligned}$$

with $\bar{p}_{I_0}(t) := \Phi(t - \tau)$ and $\tilde{g}_{I_n}(t) := \tilde{g}(t + (n-1)\tau)$ for $t \in [0, \tau]$ possess unique solutions $\bar{p}_{I_n} \in C([0, \tau]; \mathcal{H}_\omega) \cap L^2(0, \tau; \mathcal{Q})$ with $\dot{\bar{p}}_{I_n} \in L^2(0, \tau; \mathcal{Q}^*)$. The result follows by defining $\bar{p}(t) := \bar{p}_{I_n}(t + (n-1)\tau)$ for $t \in [(n-1)\tau, n\tau]$. \square

Corollary A.2. *Consider the initial trajectory problem (A.1) with $\tilde{g} \in C^1([0, T]; \mathcal{H}_\omega)$ and suppose that the history function $\Phi \in C^2([-\tau, 0]; \mathcal{H}_\omega)$ satisfies $\mathcal{K}\Phi(0) \in \mathcal{H}_\omega$ and the splicing condition*

$$(A.3) \quad \dot{\Phi}(0) + \mathcal{K}\Phi(0) = \tilde{g}(0) + \omega \dot{\Phi}(-\tau).$$

Further, let the bilinear form associated with the operator \mathcal{K} satisfy a Gårding inequality (A.2). Then the weak solution \bar{p} of (A.1) satisfies $\bar{p} \in C^1([0, T]; \mathcal{H}_\omega) \cap H^1(\mathcal{Q})$ with $\ddot{\bar{p}} \in L^2(\mathcal{Q}^)$.*

Proof. We differentiate equation (A.1a), which (formally) yields

$$(A.4a) \quad \dot{\bar{q}}(t) + \mathcal{K}\bar{q}(t) = \dot{\tilde{g}}(t) + \omega \dot{\bar{q}}(t - \tau), \quad t > 0,$$

$$(A.4b) \quad \bar{q}(t) = \dot{\Phi}(t), \quad t \in [-\tau, 0].$$

The assumptions imply $\dot{\tilde{g}} \in C([0, T]; \mathcal{H}_Q)$ and $\dot{\Phi} \in C^1([-T, 0]; \mathcal{H}_Q)$ and thus Proposition A.1 establishes the existence of a weak solution \bar{q} of (A.4). From the splicing condition (A.3) and the continuity of the weak solution \bar{p} of (A.1) we obtain

$$\dot{\bar{p}}(0^+) = -\mathcal{K}\bar{p}(0) + \tilde{g}(0) + \omega\dot{\Phi}(-\tau) = -\mathcal{K}\Phi(0) + \tilde{g}(0) + \omega\dot{\Phi}(-\tau) = \dot{\Phi}(0) = \bar{q}(0),$$

which establishes $\dot{\bar{p}} = \bar{q}$. \square

Remark A.3. If the data is sufficiently smooth and the splicing condition (A.3) is also satisfied for derivatives of the history function, i.e.,

$$\Phi^{(\ell+1)}(0) + \mathcal{K}\Phi^{(\ell)}(0) = \tilde{g}^{(\ell)}(0) + \omega\Phi^{(\ell+1)}(-\tau)$$

for $\ell \in \mathbb{N}$, then by repeating the arguments in the proof of Corollary A.2 for derivatives of \bar{p} , we obtain a smooth solution of the initial trajectory problem (A.1).

Proposition A.4. *Let (\bar{u}, \bar{p}) denote a smooth solution of the initial trajectory problem (A.1) with sufficiently smooth data. Moreover, assume that \mathcal{K} satisfies a Gårding inequality (A.2) and that the derivatives of the history function Φ and the right-hand side \tilde{g} are uniformly bounded, i.e., there exist constants C_Φ and $C_{\tilde{g}}$ such that*

$$\|\Phi^{(j)}\|_{L^\infty(-\tau, 0; \mathcal{H}_Q)}^2 \leq C_\Phi \quad \text{and} \quad \|\tilde{g}^{(j)}\|_{L^\infty(Q^*)}^2 \leq C_{\tilde{g}}.$$

Then there exists a constant C independent of τ such that

$$\|\bar{p}^{(\ell)}\|_{L^\infty(\mathcal{H}_Q)}^2 \leq \left(C_\phi + \frac{C_{\tilde{g}} T}{\kappa_Q} \right) e^{CT}$$

for all $\ell \in \mathbb{N}$. In particular, we obtain $\bar{p} \in W^{2,\infty}(\mathcal{H}_Q)$.

Proof. Using Bellman's method of steps (cf. [BZ03, Ch. 3.4]) for (A.1), we consider the sequence of PDEs

$$(A.5) \quad \langle \dot{\bar{p}}_{I_n}, q \rangle + \langle \mathcal{K}\bar{p}_{I_n}, q \rangle = \langle \omega\dot{\bar{p}}_{I_{n-1}} + \tilde{g}_{I_n}, q \rangle$$

for all test functions $q \in \mathcal{Q}$. Here, $\bar{p}_{I_n}(t) := \bar{p}(t + t_{n-1})$ for $t \in [0, \tau]$ denotes the restriction of the solution to the time interval $I_n := [t_{n-1}, t_n]$ with the the convention $\bar{p}_{I_0}(t) = \Phi(t - \tau)$ for $t \in [0, \tau]$. With the test function $q = \bar{p}_{I_n}$, the Gårding inequality (A.2), and the weighted Young's inequality we obtain

$$\begin{aligned} \frac{1}{2} \frac{d}{dt} \|\bar{p}_{I_n}\|_{\mathcal{H}_Q}^2 + \kappa_Q \|\bar{p}_{I_n}\|_{\mathcal{Q}}^2 &\leq \kappa_{\mathcal{H}_Q} \|\bar{p}_{I_n}\|_{\mathcal{H}_Q}^2 + \omega \|\dot{\bar{p}}_{I_{n-1}}\|_{\mathcal{H}_Q} \|\bar{p}_{I_n}\|_{\mathcal{H}_Q} + \|\tilde{g}_{I_n}\|_{\mathcal{Q}^*} \|\bar{p}_{I_n}\|_{\mathcal{Q}} \\ &\leq \kappa_{\mathcal{H}_Q} \|\bar{p}_{I_n}\|_{\mathcal{H}_Q}^2 + \frac{C}{2} \|\dot{\bar{p}}_{I_{n-1}}\|_{\mathcal{H}_Q}^2 + \frac{1}{2\kappa_Q} \|\tilde{g}_{I_n}\|_{\mathcal{Q}^*}^2 + \kappa_Q \|\bar{p}_{I_n}\|_{\mathcal{Q}}^2 \end{aligned}$$

with $C := \frac{\omega^2}{\kappa_Q} C_{\mathcal{Q} \hookrightarrow \mathcal{H}_Q}^2$. Absorbing $\|\bar{p}_{I_n}\|_{\mathcal{Q}}^2$, integrating over $[0, t]$, and using Grönwall's inequality yields

$$\|\bar{p}_{I_n}(t)\|_{\mathcal{H}_Q}^2 \leq e^{2\tau\kappa_{\mathcal{H}_Q}} \left(\|\bar{p}_{I_n}(0)\|_{\mathcal{H}_Q}^2 + \int_0^t \left(C \|\dot{\bar{p}}_{I_{n-1}}(s)\|_{\mathcal{H}_Q}^2 + \frac{1}{\kappa_Q} \|\tilde{g}_{I_n}(s)\|_{\mathcal{Q}^*}^2 \right) ds \right).$$

The smoothness of \bar{p} implies $\|\bar{p}_{I_n}(0)\|_{\mathcal{H}_Q}^2 = \|\bar{p}_{I_{n-1}}(0)\|_{\mathcal{H}_Q}^2 + \int_0^\tau \frac{d}{dt} \|\bar{p}_{I_{n-1}}(s)\|_{\mathcal{H}_Q}^2 ds$. Using $\frac{d}{dt} \|\bar{p}_{I_{n-1}}\|_{\mathcal{H}_Q}^2 \leq \|\dot{\bar{p}}_{I_{n-1}}\|_{\mathcal{H}_Q}^2 + \|\bar{p}_{I_{n-1}}\|_{\mathcal{H}_Q}^2$ and taking the L^∞ -norm implies

$$\begin{aligned} \|\bar{p}_{I_n}\|_{L^\infty(0, \tau; \mathcal{H}_Q)}^2 &\leq e^{2\tau\kappa_{\mathcal{H}_Q}} (1 + \tau) \|\bar{p}_{I_{n-1}}\|_{L^\infty(0, \tau; \mathcal{H}_Q)}^2 \\ &\quad + \tau \tilde{C} \|\dot{\bar{p}}_{I_{n-1}}\|_{L^\infty(0, \tau; \mathcal{H}_Q)}^2 + \frac{\tau e^{2\tau\kappa_{\mathcal{H}_Q}}}{\kappa_Q} \|\tilde{g}_{I_n}(s)\|_{L^\infty(0, \tau; \mathcal{Q}^*)}^2 \end{aligned}$$

with $\tilde{C} = e^{2\tau\kappa_{\mathcal{H}_Q}}(1 + C)$. Using the smoothness of \bar{p} , we inductively obtain

$$\begin{aligned} \|\bar{p}_{I_n}\|_{L^\infty(0,\tau;\mathcal{H}_Q)}^2 &\leq e^{2n\tau\kappa_{\mathcal{H}_Q}} \sum_{i=0}^n \binom{n}{i} (1+\tau)^{n-i} (\tau\tilde{C})^i \|\bar{p}_{I_0}^{(i)}\|_{L^\infty(0,\tau;\mathcal{H}_Q)}^2 \\ &\quad + \frac{\tau e^{2n\tau\kappa_{\mathcal{H}_Q}}}{\kappa_{\mathcal{Q}}} \sum_{i=0}^{n-1} \sum_{j=0}^i \binom{i}{j} (1+\tau)^{i-j} (\tau\tilde{C})^j \|\tilde{g}_{I_{n-i}}^{(j)}\|_{L^\infty(0,\tau;\mathcal{Q}^*)}^2. \end{aligned}$$

From $\|\Phi^{(j)}\|_{L^\infty(-\tau,0;\mathcal{H}_Q)}^2 \leq C_\Phi$ and $\|\tilde{g}^{(j)}\|_{L^\infty(\mathcal{Q}^*)}^2 \leq C_{\tilde{g}}$ for all $j \in \mathbb{N}$ and $n\tau \leq T$, we deduce

$$e^{2n\tau\kappa_{\mathcal{H}_Q}} \sum_{i=0}^n \binom{n}{i} (1+\tau)^{n-i} (\tau\tilde{C})^i \|\bar{p}_{I_0}^{(i)}\|_{L^\infty(0,\tau;\mathcal{H}_Q)}^2 \leq C_\Phi e^{(1+2\kappa_{\mathcal{H}_Q}+\tilde{C})T}.$$

Similarly, we obtain

$$\frac{\tau e^{2n\tau\kappa_{\mathcal{H}_Q}}}{\kappa_{\mathcal{Q}}} \sum_{i=0}^{n-1} \sum_{j=0}^i \binom{i}{j} (1+\tau)^{i-j} (\tau\tilde{C})^j \|\tilde{g}_{I_{n-i}}^{(j)}\|_{L^\infty(0,\tau;\mathcal{Q}^*)}^2 \leq \frac{C_{\tilde{g}} T}{\kappa_{\mathcal{Q}}} e^{(1+2\kappa_{\mathcal{H}_Q}+\tilde{C})T},$$

which implies

$$\|\bar{p}\|_{L^\infty(\mathcal{H}_Q)}^2 \leq \left(C_\Phi + \frac{C_{\tilde{g}} T}{\kappa_{\mathcal{Q}}} \right) e^{(1+2\kappa_{\mathcal{H}_Q}+\tilde{C})T}.$$

Repeating this procedure with derivatives of equation (A.5) finishes the proof. \square

[†] DEPARTMENT OF MATHEMATICS, UNIVERSITY OF AUGSBURG, UNIVERSITÄTSSTR. 14, 86159 AUGSBURG, GERMANY

E-mail address: {robert.altmann,roland.maier}@math.uni-augsburg.de

[‡] INSTITUTE OF MATHEMATICS MA 4-5, TECHNICAL UNIVERSITY BERLIN, STRASSE DES 17. JUNI 136, 10623 BERLIN, GERMANY

E-mail address: unger@math.tu-berlin.de